Electronic Supplementary Information for "Theory of polariton-assisted remote energy transfer"

Matthew Du,[a] Luis A. Martínez-Martínez,[a] Raphael F. Ribeiro,[a] Zixuan Hu,[bc] Vinod M. Menon,[de] and Joel Yuen-Zhou*[a]

[a]Department of Chemistry and Biochemistry, University of California San Diego, La Jolla, California 92093, United States.

[b]Department of Chemistry, Department of Physics, and Birck Nanotechnology Center, Purdue University, West Lafayette, IN 47907, United States.

[c]Qatar Environment and Energy Research Institute, College of Science and Engineering, HBKU, Doha, Qatar.

[d]Department of Physics, City College, City University of New York, New York 10031, United States.

[e]Department of Physics, Graduate Center, City University of New York, New York 10016, United States.

*To whom correspondence should be addressed. E-mail: joelyuen@ucsd.edu

S1 SP modes: additional details

Eq. (3a) and (5) in the main text correspond to Hamiltonians representing the SP modes and their coupling with excitons, respectively. SP modes emerge at the interface of a metal ($z<0$) and dielectric medium ($z>0$) and are assumed to be infinitely delocalized in the xy-plane (in practice, they are localized up to a coherence length, but this detail is not important for the time being). For simplicity, the dielectric medium—which contains both donor and acceptor slabs—is taken to have the same real-valued positive dielectric constant ε_d at all points within. The metal is assumed to have a Drude permittivity $\varepsilon_m(\omega)=\varepsilon_\infty-\frac{\omega_P^2}{\omega^2+i\omega\gamma}$, where ω_P is the plasma frequency, ε_∞ is the high-frequency metal permittivity, and γ is the damping constant; we set $\gamma=0$ in this formalism to get lossless modes and assume that coupling of SPs to environments that induce their relaxation processes is caused by $H_P^{(sys-B)}$ (see Eq. (3c)). Here are additional definitions for terms defined in Eqs. (3a) and (5) for each SP mode of in-plane momentum $\vec{k}$:[S1]

- The SP mode frequency is $\omega_{\vec{k}}=|\vec{k}|c\sqrt{\frac{\varepsilon_d+\varepsilon_m(\omega)}{\varepsilon_d\varepsilon_m(\omega)}}$, where c is the speed of light in vacuum.
- The evanescent decay constants for the dielectric medium and metal are given by $a_{j\vec{k}}=\sqrt{|\vec{k}|^2-\varepsilon_j(\omega_{\vec{k}})\,(\omega_{\vec{k}}/c)^2}$, where $j=d,m$.
- The $\vec{k}$-dependent quantization length is $L_{\vec{k}}=\frac{-\varepsilon_m}{|a_{d\vec{k}}|}+\frac{1}{2|a_{m\vec{k}}|}\left[\frac{d(\omega\varepsilon_m(\omega))}{d\omega}\bigg|_{\omega=\omega_{\vec{k}}}\left(\frac{\varepsilon_m-\varepsilon_d}{\varepsilon_m}\right)-\varepsilon_m-\varepsilon_d\right]$. It was previously reported in the literature[S2] with an additional factor of $\frac{1}{2}$; we believe our displayed expression here is correct (see SI in[S3]).

The formalism associated with Eq. (5) has been previously utilized in other contexts.[S3–S6]

S2 Case i

S2.1 Derivation of EET rate Eq. (7)

Here we derive Eq. (7) of the main text by following works of Sumi[S7] and Cao.[S8] This formula describes the rate of transfer from eigenstate $|I\rangle$ to eigenstate $|F\rangle$ of $H_{sys}^{(i)}$ due to perturbation $V^{(i)}$ (Section 2.1), where $|I\rangle$ and $|F\rangle$ are excitonic/polaritonic states for the donor and acceptor, respectively.

For notational simplicity, we define for this derivation H_D' and H_A' to be the donor and acceptor Hamiltonian, respectively, such that $H_C'=H_C+H_P+H_{CP}$ for the chromophore C that is strongly coupled to a SP mode and $H_{C'}'=H_{C'}$ for the other chromophore C', which is weakly coupled to all SP modes. We also introduce the definitions $H_C'^{(sys/B)}=H_C{}^{(sys/B)}+H_P^{(sys/B)}$ and $H_{C'}'^{(sys/B)}=H_{C'}^{(sys/B)}$. Then we note for clarity that $H_A'^{(sys)}|I\rangle=H_D'^{(sys)}|F\rangle=0$. In addition, $H_0^{(i)}=H_D'+H_A'$ has eigenstates $\{|\mathscr{D}\rangle\}$ ($\{|\mathscr{A}\rangle\}$) that are also eigenstates of H_D' (H_A') and whose excitonic/polaritonic-system component represents *only* donor (acceptor) but bath component represents *all* of donor, acceptor, and SPs.

Assuming excitation of donor followed by thermal equilibration occurs before EET, the initial density matrix of the system and bath is assumed to be $\rho_0=\rho_D^{(sys-B)}\rho_A^{(B)}=\sum_{\mathscr{D}}p_{0,\mathscr{D}}|\mathscr{D}\rangle\langle\mathscr{D}|$, where $p_{0,\mathscr{D}}$ is the equilibrium occupation probability of system-bath state $|\mathscr{D}\rangle$. The constituent density matrices $\rho_D^{(sys-B)}=\frac{e^{-H_D'/k_BT}}{\mathrm{tr}e^{-H_D'/k_BT}}$ and $\rho_A^{(B)}=\frac{e^{-H_A'^{(B)}/k_BT}}{\mathrm{tr}e^{-H_A'^{(B)}/k_BT}}$ respectively represent the pre-EET equilibrium distribution of donor excited vibronic and acceptor ground vibrational states, in corresponding tensor products with photon states. Then the rate of transfer from $|I\rangle$ to $|F\rangle$ given by Fermi's golden rule (FGR) is

$$\gamma_{F\leftarrow I}=\frac{2\pi}{\hbar}\sum_{\mathscr{D},\mathscr{A}}p_{0,\mathscr{D}}|\langle\mathscr{P}_F\mathscr{A}|V^{(i)}|\mathscr{P}_I\mathscr{D}\rangle|^2\delta(\hbar\omega_{\mathscr{A},\mathscr{D}}),\tag{S1}$$

The state $|\mathscr{P}_I\mathscr{D}\rangle$ ($|\mathscr{P}_F\mathscr{A}\rangle$) results from projection $\mathscr{P}_I=|I\rangle\langle I|$ ($\mathscr{P}_F=|F\rangle\langle F|$) of the system component of $|\mathscr{D}\rangle$ ($|\mathscr{A}\rangle$) onto $|I\rangle$ ($|F\rangle$). To express this equation in the (purely electronic/polaritonic) eigenbasis $\{|D\rangle\}\cup\{|A\rangle\}$ of $H_{sys}^{(i)}$, we first use the fact that the bath modes on each type of chromophore are independent (see Eqs. (2b) and (2c)) and write the time-domain expression:

$$\begin{aligned}\gamma_{F\leftarrow I}&=\frac{1}{\hbar^2}\int_{-\infty}^{\infty}dt\sum_{\mathscr{D},\mathscr{A}}p_{0,\mathscr{D}}\langle\mathscr{P}_I\mathscr{D}|V^{(i)}|\mathscr{P}_F\mathscr{A}\rangle\langle\mathscr{P}_F\mathscr{A}|e^{-iH_0^{(i)}t/\hbar}V^{(i)}e^{iH_0^{(i)}t/\hbar}|\mathscr{P}_I\mathscr{D}\rangle\\&=\frac{1}{\hbar^2}\int_{-\infty}^{\infty}dt\sum_{\mathscr{D}}p_{0,\mathscr{D}}\langle\mathscr{P}_I\mathscr{D}|V^{(i)}\,\mathscr{P}_Fe^{-i(H_A'+H_D'^{(B)})t/\hbar}V^{(i)}\,e^{i(H_D'+H_A'^{(B)})t/\hbar}|\mathscr{P}_I\mathscr{D}\rangle,\end{aligned}\tag{S2}$$

where in the second line, we have used $\sum_{\mathscr{A}}|\mathscr{P}_F\mathscr{A}\rangle\langle\mathscr{P}_F\mathscr{A}|e^{-iH_0^{(i)}t/\hbar}=\mathscr{P}_Fe^{-i(H_A'+H_D'^{(B)})t/\hbar}$ and $e^{iH_0^{(i)}t/\hbar}|\mathscr{P}_I\mathscr{D}\rangle=e^{i(H_D'+H_A'^{(B)})t/\hbar}|\mathscr{P}_I\mathscr{D}\rangle$. Using the independence of the D,A vibrational bath modes, we obtain

$$\gamma_{F\leftarrow I}=\frac{1}{\hbar^2}\int_{-\infty}^{\infty}dt\sum_{D'}\sum_{A'}V_{IF}^{(i)}V_{D'A'}^{(i)*}\mathrm{tr}_{bD}\{e^{-iH_D'^{(B)}t/\hbar}\langle D'|e^{iH_D't/\hbar}\mathscr{P}_I\rho_D^{(sys-B)}|I\rangle\}\mathrm{tr}_{bA}\{e^{iH_A'^{(B)}t/\hbar}\rho_A^{(B)}\langle F|e^{-iH_A't/\hbar}|A'\rangle\}\tag{S3}$$

for $V^{(i)}_{D'A'} = \langle D'|V^{(i)}|A'\rangle$; here, tr_{bC} denotes a trace over the bath degrees of freedom associated with C. In the limit of weak exciton-bath coupling, $[e^{iH'_D t/\hbar}, \mathscr{P}_I] \approx 0$, and $\langle D'|e^{iH'_D t/\hbar}\rho_D^{(sys-B)}|I\rangle \approx 0$ ($\langle F|e^{-iH'_A t/\hbar}|A'\rangle \approx 0$) for $D' \neq I$ ($A' \neq F$). Then

$$\gamma_{F\leftarrow I} \approx \frac{1}{\hbar^2}|V^{(i)}_{FI}|^2 \int_{-\infty}^{\infty} dt\, \mathrm{tr}_{bD}\{e^{-iH_D^{\prime(B)}t/\hbar}\langle I|e^{iH'_D t/\hbar}\rho_D^{(sys-B)}|I\rangle\}\mathrm{tr}_{bA}\{e^{iH_A^{\prime(B)}t/\hbar}\rho_A^{(B)}\langle F|e^{-iH'_A t/\hbar}|F\rangle\}. \tag{S4}$$

To proceed further, let us define the quantities

$$\mathscr{I}_F(\omega) = \frac{1}{2\pi}\int_{-\infty}^{\infty} dt\, e^{i\omega t}\mathrm{tr}_{bA}\{e^{iH_A^{\prime(B)}t/\hbar}\rho_A^{(B)}\langle F|e^{-iH'_A t/\hbar}|F\rangle\}, \tag{S5}$$

$$\mathscr{E}_I(\omega) = \frac{1}{2\pi}\int_{-\infty}^{\infty} dt\, e^{-i\omega t}\mathrm{tr}_{bD}\{e^{-iH_D^{\prime(B)}t/\hbar}\langle I|e^{iH'_D t/\hbar}\rho_D^{(sys-B)}|I\rangle\}, \tag{S6}$$

representing the spectra for absorption of acceptor state F and emission of donor state I, respectively. Also, denote the corresponding spectral overlap as

$$J_{F,I} = \frac{1}{\hbar}\int_{-\infty}^{\infty} d\omega\, \mathscr{E}_I(\omega)\mathscr{I}_F(\omega). \tag{S7}$$

Eq. (S4) then yields,

$$\gamma_{F\leftarrow I} \approx \frac{2\pi}{\hbar}|V^{(i)}_{FI}|^2 J_{F,I}, \tag{S8}$$

which is Eq. (7) of the main text; in other words, the spectral overlap $J_{F,I}$ takes on the role of a density of final states for a FGR rate. We note that for our simulations where the donors and acceptors are reversed (see Sections 3 and S2.9), Eq. (S8) still applies except D,I (A,F) now refer to acceptors (donors).

S2.2 Estimation of spectral overlaps

As an illustration of the application of our theory, in this subsection, we develop a simplified Lorentzian overlap model to compute $J_{F,I}$ at temperature $T = 0$. To write Eqs. (S5) and (S6) as Lorentzian lineshapes, we follow a Feshbach projection operator approach.[S9–S12] While we proceed with the specific case of only donors strongly coupled to a SP (*i.e.*, $H'_A = H_A$ and $H'_D = H_D + H_P + H_{DP}$), the derivation can be readily extended to the case of acceptors strongly coupled to a SP.

Define the projectors

$$\mathscr{P}_A = \sum_{l,m}|A_{lm}\rangle\langle A_{lm}| \otimes |0_B\rangle\langle 0_B|, \tag{S9}$$

$$\mathscr{P}_D = \sum_{i,j}|D_{ij}\rangle\langle D_{ij}| \otimes |0_B\rangle\langle 0_B| + \sum_{\vec{k}\in \mathrm{FBZ}}|\vec{k}\rangle\langle\vec{k}| \otimes |0_B\rangle\langle 0_B| \tag{S10}$$

($|0_B\rangle$ is the vacuum state for chromophores and SP bath modes, and $|\vec{k}\rangle = a^\dagger_{\vec{k}}|0\rangle$), which map vibronic (possibly including photonic component) states onto electronic/photonic—*i.e.*, "bathless"—states. Let the identity on the entire set of degrees of freedom be 1_{sys-B} and define the projectors $\mathscr{Q}_A = 1_{sys-B} - \mathscr{P}_A$ and $\mathscr{Q}_D = 1_{sys-B} - \mathscr{P}_D$. Then the time-dependent Schrödinger equation $\frac{d}{dt}|\psi(t)\rangle = -\frac{i}{\hbar}H'_C|\psi(t)\rangle$ for $C = D,A$ can be rewritten as the coupled equations

$$-\frac{i}{\hbar}\mathscr{P}_C H'_C \mathscr{P}_C|\mathscr{P}_C\psi(t)\rangle - \frac{i}{\hbar}\mathscr{P}_C H'_C \mathscr{Q}_C|\mathscr{Q}_C\psi(t)\rangle = \frac{d}{dt}|\mathscr{P}_C\psi(t)\rangle, \tag{S11a}$$

$$-\frac{i}{\hbar}\mathscr{Q}_C H'_C \mathscr{P}_C|\mathscr{P}_C\psi(t)\rangle - \frac{i}{\hbar}\mathscr{Q}_C H'_C \mathscr{Q}_C|\mathscr{Q}_C\psi(t)\rangle = \frac{d}{dt}|\mathscr{Q}_C\psi(t)\rangle. \tag{S11b}$$

After the initial condition $|\mathscr{Q}_C\psi(0)\rangle = 0$ (which holds at $T = 0$), multiplying both sides of Eq. (S11) by $\Theta(t)$, and plugging the formal solution of Eq. (S11b) into Eq. (S11a), we obtain the Green functions $G_C(t) = \Theta(t)e^{-iH'_C t/\hbar}$ which can be Fourier transformed as,[S11]

$$G_A(\hbar\omega) = -i\int_{-\infty}^{\infty} dt\, e^{i\omega t}G_A(t) = \lim_{\varepsilon\to 0^+}\frac{1}{\hbar\omega - H_A^{(sys)}\otimes|0_B\rangle\langle 0_B| - R_A(\hbar\omega) + i\varepsilon}, \tag{S12a}$$

$$G_D(\hbar\omega) = -i\int_{-\infty}^{\infty} dt\, e^{i\omega t}G_D(t) = \lim_{\varepsilon\to 0^+}\frac{1}{\hbar\omega - (H_D^{(sys)} + H_P^{(sys)} + H_{DP})\otimes|0_B\rangle\langle 0_B| - R_{DP}(\hbar\omega) + i\varepsilon}, \tag{S12b}$$

where

$$R_A(\hbar\omega) = \mathscr{P}_A H_A^{(sys-B)} \mathscr{Q}_A \frac{1}{\hbar\omega - \mathscr{Q}_A H'_A \mathscr{Q}_A + i\varepsilon} \mathscr{Q}_A H_A^{(sys-B)} \mathscr{P}_A, \tag{S13a}$$

$$R_D(\hbar\omega) = \mathscr{P}_D[H_D^{(sys-B)} + H_P^{(sys-B)}]\mathscr{Q}_D \frac{1}{\hbar\omega - \mathscr{Q}_D H'_D \mathscr{Q}_D + i\varepsilon} \mathscr{Q}_D[H_D^{(sys-B)} + H_P^{(sys-B)}]\mathscr{P}_D, \tag{S13b}$$

are the so-called self-energy terms. We next make the partition $R_C(\hbar\omega) = \mathrm{Re}R_C(\hbar\omega) - \frac{i}{2}\Gamma_C(\hbar\omega)$ with $\Gamma_C(\hbar\omega) = -2\mathrm{Im}R_C(\hbar\omega)$ and assume that the Lamb shifts $\mathrm{Re}R_C(\hbar\omega)$ contribute insignificantly when compared to the exciton/SP energies and can thus be neglected. In addition, we take the wide-band approximation that all (diagonal) matrix elements of $\Gamma_C(\hbar\omega)$ are constant as a function of ω: $\langle A_{lm}, 0_B|\Gamma_A(\hbar\omega)|A_{lm}, 0_B\rangle \approx \Gamma_A$, $\langle D_{ij}, 0_B|\Gamma_D(\hbar\omega)|D_{ij}, 0_B\rangle \approx \Gamma_D$, and $\langle 1_{\vec{k}}, 0_B|\Gamma_D(\hbar\omega)|1_{\vec{k}}, 0_B\rangle \approx \Gamma_{P,\vec{k}}$. Then explicitly writing out the respective Hamiltonians in Eq. (S12), we arrive at

$$G_A(\hbar\omega) = \lim_{\varepsilon\to 0^+} \frac{1}{\hbar\omega - (\hbar\omega_A - \frac{i}{2}\Gamma_A)\sum_{l,m}|A_{lm}\rangle\langle A_{lm}| \otimes |0_B\rangle\langle 0_B| + i\varepsilon} \tag{S14a}$$

$$G_D(\hbar\omega) = \lim_{\varepsilon\to 0^+} \frac{1}{\hbar\omega - [(\hbar\omega_D - \frac{i}{2}\Gamma_D)\sum_{i,j}|D_{ij}\rangle\langle D_{ij}| + \sum_{\vec{k}\in \mathrm{FBZ}}(\hbar\omega_{\vec{k}} - \frac{i}{2}\Gamma_{P,\vec{k}})a^\dagger_{\vec{k}}a_{\vec{k}} + H_{DP}] \otimes |0_B\rangle\langle 0_B| + i\varepsilon} \tag{S14b}$$

$$= \lim_{\varepsilon\to 0^+} \frac{1}{\hbar\omega - [(\hbar\omega_D - \frac{i}{2}\Gamma_D)\sum_{\vec{k}\in \mathrm{FBZ}}\sum_d |d_{\vec{k}}\rangle\langle d_{\vec{k}}| + \sum_{\vec{k}\in \mathrm{FBZ}}\sum_\alpha(\hbar\omega_{\alpha_{D,\vec{k}}} - \frac{i}{2}\Gamma_{\alpha_{D,\vec{k}}})|\alpha_{D,\vec{k}}\rangle\langle\alpha_{D,\vec{k}}|] \otimes |0_B\rangle\langle 0_B| + i\varepsilon}. \tag{S14c}$$

It is intuitively clear that the terms in brackets in the denominators of Eqs. (S14b) and (S14c) correspond to effective Hamiltonians of the donor-SP coupled system. In fact, $\hbar\omega_{\alpha_{D,\vec{k}}}$ and $\Gamma_{\alpha_{D,\vec{k}}}$ are the resulting (real-valued) energy and linewidth of $|\alpha_{D,\vec{k}}\rangle$ (defined just after Eq. (6) in the main text) for $\alpha = \mathrm{UP}, \mathrm{LP}$. Comparing those two equations shows that not only can the polariton energies and linewidths be obtained from the diagonalization of a non-Hermitian Hamiltonian for the donors and SP modes, but all dark states have the same energy and linewidth as the bare chromophores.

More precisely, applying the assumption of weak system-bath coupling that was used to derive Eq. (7) and setting $\rho_C^{(B)} = |0_B\rangle\langle 0_B|$ ($T = 0$), we can readily relate the expressions for absorption and emission spectra (Eqs. (S5) and (S6), respectively) to matrix elements of the Green's functions (see Eq. (S12)),

$$\begin{aligned}\mathscr{I}_F(\omega) &\approx \frac{1}{2\pi}\mathrm{tr}_{bA}\{\rho_A^{(B)}\langle F| - 2\mathrm{Im}G_A(\hbar\omega)|F\rangle\} \\ &= \frac{1}{\pi}\frac{\frac{1}{2}\Gamma_F}{(\hbar\omega - \hbar\omega_F)^2 + (\frac{1}{2}\Gamma_F)^2},\end{aligned} \tag{S15a}$$

$$\begin{aligned}\mathscr{E}_I(\omega) &\approx \frac{1}{2\pi}\mathrm{tr}_{bD}\{\rho_D^{(B)}\langle I| - 2\mathrm{Im}G_D(\hbar\omega)|I\rangle\} \\ &= \frac{1}{\pi}\frac{\frac{1}{2}\Gamma_I}{(\hbar\omega - \hbar\omega_I)^2 + (\frac{1}{2}\Gamma_I)^2},\end{aligned} \tag{S15b}$$

with $F = A$ ($I = \alpha_{D,\vec{k}}, D$) representing any state of type $|A_{lm}\rangle$ ($|\alpha_{\vec{k},D}\rangle, |d_{\vec{k}}\rangle$), and we thus obtain the Lorentzian spectral overlap $J_{F,I} = \frac{1}{\pi}\frac{\frac{\Gamma_I+\Gamma_F}{2}}{(\frac{\Gamma_I+\Gamma_F}{2})^2+(\hbar\omega_{FI})^2}$.

Although we made several approximations to achieve this form, Lorentzian behavior is usually characteristic of lineshapes near their peaks,[S13] leading to overlaps and thus EET rates that are especially relevant when initial and final states are near resonance. In passing, we mention that a different physical mechanism to obtain Lorentzian lineshapes occurs when electronic states are coupled to overdamped Brownian oscillators in the limits of high temperature and fast nuclear dynamics[S11].

S2.3 Lack of supertransfer enhancement

Here, we demonstrate that even though the donor polariton state is coherently delocalized, the superradiance enhancement of EET to bare acceptors that one could expect[S14,S15] is negligible when taking into account the distance dependence and orientational correlation of the involved dipolar interactions. The essence of supertransfer is that a constructive interference of individual donor dipoles in an aggregate can lead to FRET rates that scale as N times a bare FRET rate. However, for this to happen, it is important to have a geometric arrangement where all donors are equally coupled to, *i.e.*, equidistantly spaced and identically oriented with respect to, all acceptors;

this is not the case in our problem.

To show this point explicitly, we first evaluate the FRET rate associated with the delocalized donor $|D_{\vec{k}=0}\rangle$ transferring energy to bare acceptors,

$$\begin{aligned}\gamma^{FRET}_{A\leftarrow D_{\vec{k}=0}} &\equiv \frac{2\pi}{\hbar}\sum_{l,m}|\langle A_{lm}|H_{DA}|D_{\vec{k}=\vec{0}}\rangle|^2 J_{A,D_{\vec{k}=\vec{0}}} \\ &\approx \frac{2\pi}{\hbar}\mu_D^2\mu_A^2\sum_{l,m}\frac{1}{N_D}\left(\sum_{i,j}\frac{\kappa_{ijlm}}{r^3_{ijlm}}\right)^2 J_{A,D_{\vec{k}=\vec{0}}},\end{aligned} \tag{S16}$$

where we have approximated $|D_{\vec{k}=0}\rangle$ as a totally symmetric state across all chromophores, $|c_{D_{i'j'}D_{\vec{k}=0}}|^2 = \frac{|\kappa_{\vec{k}D_{i'j'}}|^2}{\sum_{i,j}|\kappa_{\vec{k}D_{ij}}|^2} \approx \frac{1}{N_D}$ (see definition of $|C_{\vec{k}}\rangle$ for $C = D,A$ in main text right after Eq. (6)).

Compare Eq. (S16) to the corresponding supertransfer rate

$$\begin{aligned}\gamma_{\text{supertransfer}} &= \frac{2\pi}{\hbar}\mu_D^2\mu_A^2\frac{1}{N_D}\sum_{l,m}\left|\sum_{i,j}V_{lm}\right|^2 J_{A,D} \\ &= \frac{2\pi}{\hbar}\mu_D^2\mu_A^2\sum_{l,m}N_D V_{lm}^2 J_{A,D},\end{aligned} \tag{S17}$$

where V_{lm} is the identical coupling between acceptor A_{lm} and any donor D_{ij} for all i,j and may take on any nonzero real value. Since the separations between the donors and any given acceptor are clearly different in the slab geometry of this work, the resulting rate is much less than that of Eq. (S17).

We next show this more precisely. Consider $S^{(lm)}_{>}(\varepsilon) = \left\{(i,j)\,\middle|\,\frac{4}{r^6_{ijlm}} \geq \varepsilon^2 V_{lm}^2\right\}$ for positive $\varepsilon \to 0$, where this set has $N^{(lm)}_{>}$ elements. Then

$$\frac{1}{N_D}\left(\sum_{i,j}\frac{\kappa^2_{ijlm}}{r^3_{ijlm}}\right)^2 \leq \frac{1}{N_D}\left(\sum_{(i,j)\in S^{(lm)}_{>}(\varepsilon)}\frac{4}{r^3_{ijlm}}\right)^2 + \frac{2}{N_D}\left(\sum_{(i,j)\in S^{(lm)}_{>}(\varepsilon)}\frac{2}{r^3_{ijlm}}\right)\left(\sum_{(i,j)\notin S^{(lm)}_{>}(\varepsilon)}\frac{2}{r^3_{ijlm}}\right) + \frac{1}{N_D}\left(\sum_{(i,j)\notin S^{(lm)}_{>}(\varepsilon)}\frac{4}{r^3_{ijlm}}\right)^2.$$

We have used the fact that the squared FRET orientation factor κ^2_{ijlm} ranges from 0 to 4.[S16] Since $S^{(lm)}_{>}(\varepsilon)$ is a finite set, the first term on the righthand side vanishes for sufficiently large N_D. Thus,

$$\frac{1}{N_D}\left(\sum_{i,j}\frac{\kappa^2_{ijlm}}{r^3_{ijlm}}\right)^2 \leq \frac{2(N_D - N^{(lm)}_{>})\varepsilon|V_{lm}|}{N_D}\sum_{(i,j)\in S^{(lm)}_{>}(\varepsilon)}\frac{2}{r^3_{ijlm}} + \frac{(N_D - N^{(lm)}_{>})^2\varepsilon^2 V^2_{lm}}{N_D},$$

and so

$$\frac{\gamma^{FRET}_{A\leftarrow D_{\vec{k}=0}}}{\gamma_{\text{supertransfer}}} \leq \frac{J_{A,D_{\vec{k}=\vec{0}}}\sum_{l,m}\left[\frac{2(N_D-N^{(lm)}_{>})\varepsilon|V_{lm}|}{N_D}\sum_{(i,j)\in S^{(lm)}_{>}(\varepsilon)}\frac{2}{r^3_{ijlm}} + \frac{(N_D-N^{(lm)}_{>})^2\varepsilon^2V^2_{lm}}{N_D}\right]}{J_{A,D}N_D\sum_{l,m}V^2_{lm}}.$$

In the limit $N_D \to \infty$, we find

$$\frac{\gamma^{FRET}_{A\leftarrow D_{\vec{k}=0}}}{\gamma_{\text{supertransfer}}} \to \frac{J_{A,D_{\vec{k}=\vec{0}}}\varepsilon^2}{J_{A,D}} \to 0.$$

Therefore, we conclude that the decay of dipolar interactions with respect to distance precludes a supertransfer enhancement[S14,S15] in our problem.

By noticing that $\left|\sum_{i,j}\frac{\kappa_{ijlm}}{r^3_{ijlm}}\right|^2 > \sum_{i,j}\frac{\kappa^2_{ijlm}}{r^6_{ijlm}}$ (at least when all $\kappa_{ijlm} \geq 0$), and for $J_{A,D} \approx J_{A,D_{\vec{k}=\vec{0}}}$, we still expect a coherence enhancement of EET: $\gamma^{FRET}_{A\leftarrow D_{\vec{k}=0}} > \frac{2\pi}{\hbar}\mu_D^2\mu_A^2\sum_{l,m}\frac{1}{N_D}\sum_{i,j}\frac{\kappa^2_{ijlm}}{r^6_{ijlm}}J_{A,D}$, the corresponding bare FRET rate. However, this enhancement is quite modest compared to all other effects that we consider in our problem (*e.g.*, PRET contributions).

S2.4 Derivation of rate Eq. (12a) from donor polaritons to acceptors

Here, we derive expressions for EET rates between a multi-layer slab of $N_D \gg N_{xy,D}$ donor molecules strongly coupled to a SP and a monolayer of acceptor molecules at $z = z_{0,A} > z_{j,D}$ for all j. The polariton states $\alpha = \mathrm{UP}, \mathrm{LP}$ are of the form $|\alpha_{D,\vec{k}}\rangle = c_{D_{\vec{k}}\alpha_{D,\vec{k}}}|D_{\vec{k}}\rangle + c_{\vec{k}\alpha_{D,\vec{k}}}|\vec{k}\rangle$, where $|\vec{k}\rangle = a^\dagger_{\vec{k}}|0\rangle$ and

$$|D_{\vec{k}}\rangle = \frac{1}{\sqrt{\sum_{i,j}|\kappa_{\vec{k}D_{ij}}|^2 e^{-2a_{d\vec{k}}z_{j,D}}}} \sum_{i,j} \kappa_{\vec{k}D_{ij}} e^{-a_{d\vec{k}}z_{j,D}} e^{i\vec{k}\cdot\vec{R}_{i,D}} |D_{ij}\rangle. \tag{S18}$$

Plugging Eq. (S18) into Eq. (8a), the rate of transfer from donor polariton state $|\alpha_{D,\vec{k}}\rangle$ ($\alpha = \mathrm{UP}, \mathrm{LP}$) to acceptors is

$$\begin{aligned}
\gamma_{A\leftarrow\alpha_{D,\vec{k}}} &= \frac{2\pi}{\hbar}\sum_l \left|\langle A_{l0}|H_{DA}+H_{AP}|\alpha_{D,\vec{k}}\rangle\right|^2 J_{A\alpha_{D,\vec{k}}} \\
&= \frac{2\pi}{\hbar}\sum_l \left|\langle A_{l0}|H_{DA}+H_{AP}|\left(c_{D_{\vec{k}}\alpha_{D,\vec{k}}}\sum_{i,j}\frac{\kappa_{\vec{k}D_{ij}}e^{-a_{d\vec{k}}z_{j,D}}e^{i\vec{k}\cdot\vec{R}_{i,D}}}{\sqrt{\sum_{i,j}|\kappa_{\vec{k}D_{ij}}|^2 e^{-2a_{d\vec{k}}z_{j,D}}}}|D_{ij}\rangle + c_{\vec{k}\alpha_{D,\vec{k}}}|\vec{k}\rangle\right)\right|^2 J_{A,\alpha_{D,\vec{k}}}.
\end{aligned} \tag{S19}$$

For simplicity, we next assume the chromophores lie in an infinitely extended and translationally invariant slab along the xy plane and their TDMs are isotropically distributed and orientationally uncorrelated:

$$\begin{aligned}
\gamma_{A\leftarrow\alpha_{D,\vec{k}}} &= |c_{D_{\vec{k}}\alpha_{D,\vec{k}}}|^2 \frac{2\pi}{\hbar} N_A \sum_{i,j}\left(\frac{e^{-2a_{d\vec{k}}z_j}}{N_{xy,D}\sum_j e^{-2a_{d\vec{k}}z_{j,D}}}\right)\frac{\mu_D^2\mu_A^2\langle\kappa^2_{FRET}\rangle}{r_{ij}^6} J_{A\alpha_{D,\vec{k}}} \\
&\quad + |c_{\vec{k}\alpha_{D,\vec{k}}}|^2 \frac{2\pi}{\hbar}\rho_A^{(2D)}\mu_A^2\langle|\kappa_{LM,\vec{k}}|^2\rangle\frac{\hbar\omega_{\vec{k}}}{2\varepsilon_0 L_{\vec{k}}} e^{-2a_{d\vec{k}}z_{0,A}} J_{A\alpha_{D,\vec{k}}},
\end{aligned} \tag{S20a}$$

where r_{ij} is distance between acceptor at $(0,0,z_{0,A})$ and donor ij, $\rho_A^{(2D)} = \frac{N_{xy,A}}{S}$ is the concentration of acceptors per unit area, the isotropically averaged orientation factors for FRET and light-matter interaction are $\langle\kappa^2_{FRET}\rangle = \langle\kappa^2_{ijl0}\rangle = \frac{2}{3}$ [S16], and $\langle|\kappa_{LM,\vec{k}}|^2\rangle = \langle|\kappa_{\vec{k}D_{ij}}|^2\rangle = \frac{2}{3} + \frac{1}{3}\frac{|\vec{k}|^2}{a^2_{d\vec{k}}}$ [S4]. Eq. (S20a) shows that the isotropic distribution of dipoles and the lack of correlations amongst their orientations yields an incoherently averaged rate over the populations of exciton (first term) and SP (second term). Furthermore, Eq. (13b) of the main text is a less explicit form of Eq. (S20a) that follows from using the approximation $\frac{e^{-2a_{d\vec{k}}z_{j,D}}}{N_{xy,D}\sum_j e^{-2a_{d\vec{k}}z_{j,D}}} \approx |c_{D_{ij}D_{\vec{k}}}|^2 = \frac{|\kappa_{\vec{k}D_{ij}}|^2 e^{-2a_{d\vec{k}}z_{j,D}}}{\sum_{i,j}|\kappa_{\vec{k}D_{ij}}|^2 e^{-2a_{d\vec{k}}z_{j,D}}}$ (*i.e.*, ignoring the orientational dependence of the exciton populations).

In obtaining Eq. (S20a), we have utilized the following approximations which are valid for large N_D:

$$\left\langle \frac{\kappa_{\vec{k}D_{ij}}\kappa_{ijl0}\kappa^*_{\vec{k}D_{i'j'}}\kappa_{i'j'l0}}{\sum_{i,j}|\kappa_{\vec{k}D_{ij}}|^2 e^{-2a_{d\vec{k}}z_{j,D}}}\right\rangle \approx \frac{\langle\kappa_{\vec{k}D_{ij}}\kappa_{ijl0}\kappa^*_{\vec{k}D_{i'j'}}\kappa_{i'j'l0}\rangle}{\sum_{i,j}\langle|\kappa_{\vec{k}D_{ij}}|^2\rangle e^{-2a_{d\vec{k}}z_{j,D}}} = \frac{\langle\kappa_{\vec{k}D_{ij}}\kappa_{ijl0}\kappa^*_{\vec{k}D_{i'j'}}\kappa_{i'j'l0}\rangle}{\langle|\kappa_{LM}|^2\rangle N_{xy,D}\sum_j e^{-2a_{d\vec{k}}z_{j,D}}}, \tag{S21a}$$

$$\left\langle \frac{\kappa_{\vec{k}D_{ij}}\kappa_{ijlm}\kappa^*_{\vec{k}A_{l0}}}{\sqrt{\sum_{i,j}|\kappa_{\vec{k}D_{ij}}|^2 e^{-2a_{d\vec{k}}z_{j,D}}}}\right\rangle \approx \frac{\langle\kappa_{\vec{k}D_{ij}}\kappa_{ijlm}\kappa^*_{\vec{k}A_{l0}}\rangle}{\langle\sqrt{\sum_{i,j}|\kappa_{\vec{k}D_{ij}}|^2 e^{-2a_{d\vec{k}}z_{j,D}}}\rangle}. \tag{S21b}$$

In addition, we have applied a mean-field approach to the orientational factors,

$$\langle\kappa_{\vec{k}D_{ij}}\kappa_{ijl0}\kappa^*_{\vec{k}D_{i'j}}\kappa_{i'j'l0}\rangle \approx \langle\kappa_{\vec{k}D_{ij}}\kappa^*_{\vec{k}D_{i'j}}\rangle\langle\kappa_{ijl0}\kappa_{i'j'l0}\rangle = \langle|\kappa_{LM,\vec{k}}|^2\rangle\langle\kappa^2_{FRET}\rangle\delta_{(i,j),(i'j')}, \tag{S22a}$$

$$\langle\kappa_{\vec{k}D_{ij}}\kappa_{ijl0}\kappa^*_{\vec{k}A_{l0}}\rangle \approx \langle\kappa_{\vec{k}D_{ij}}\kappa^*_{\vec{k}A_{l0}}\rangle\langle\kappa_{ijl0}\rangle = 0. \tag{S22b}$$

In the continuum limit, Eq. (S20a) reads,

$$\gamma_{A\leftarrow\alpha_{D,\vec{k}}} = \frac{2\pi}{\hbar}\rho_A^{(2D)}\left[|c_{D_{\vec{k}}a_{D,\vec{k}}}|^2\mu_D^2\mu_A^2\langle\kappa^2_{FRET}\rangle\frac{\int_s^{s+\mathscr{W}} dz e^{-2a_{d\vec{k}}z}\frac{\pi}{2(z_{0,A}-z)^4}}{\frac{e^{-2a_{d\vec{k}}(s+\mathscr{W})}-e^{-2a_{d\vec{k}}s}}{-2a_{d\vec{k}}}} + |c_{\vec{k}\alpha_{D,\vec{k}}}|^2\mu_A^2\langle|\kappa_{LM,\vec{k}}|^2\rangle\frac{\hbar\omega_{\vec{k}}}{2\varepsilon_0 L_{\vec{k}}}e^{-2a_{d\vec{k}}z_{0,A}}\right] J_{A\alpha_{D,\vec{k}}}, \tag{S23}$$

where the base of the donor slab is located at $z = s$ and its thickness is $\mathscr{W}$ (while the integral over z has an analytical solution, it is complicated and does not shed much insight into the problem).

S2.5 Derivation of rate Eq. (12b) from donor dark states to acceptors

Here, we show that the rate (Eq. (8b)) of EET from donor dark states to a spatially separated monolayer of bare acceptors at $z = z_{0,A}$ converges to the bare FRET rate $\gamma_{\text{bare FRET}}$ in Eq. (12b) assuming that $N_D \gg N_{xy,D}$ and all donor and acceptor TDMs are isotropically oriented and uncorrelated. The steps applied in this subsection can be extended in a straightforward manner to establish this result for multiple layers in the acceptor slab. This result is intuitively expected given that the dark states are purely excitonic and centered at the original transition frequency ω_D; furthermore, the density of dark states is close to the original density of bare donor states. Our derivation here relies on Lorentzian lineshapes for the dark donor and acceptor states (see Section S2.2); however, we anticipate the conclusions to hold for more general lineshapes under certain limits.

As suggested by Section S2.2 and the main text, we assume that the lineshape of each dark state $|d_{D,\vec{k}}\rangle$ can be expressed as a Lorentzian with peak energy and linewidth identical to that of bare donors, leading to $J_{A,d_{D,\vec{k}}} = J_{A,D}$. Connecting this finding to the relevant rate expression, we can rewrite Eq. (8b) of the main text for an acceptor monolayer as

$$\gamma_{A\leftarrow dark_D} = \frac{2\pi}{\hbar}\frac{1}{N_D - N_{xy,D}}\sum_l \left[\sum_{i,j}|\langle A_{l0}|H_{DA}|D_{ij}\rangle|^2 - \sum_{\vec{k}\in \text{FBZ}}|\langle A_{l0}|H_{DA}|D_{\vec{k}}\rangle|^2\right] J_{A,D}. \tag{S24}$$

We have used the relation $\sum_{\vec{k}\in\text{FBZ}}\sum_d |d_{\vec{k}}\rangle\langle d_{\vec{k}}| = 1_D^{(sys)} - \sum_{\vec{k}\in\text{FBZ}}|D_{\vec{k}}\rangle\langle D_{\vec{k}}|$ for donor (electronic) identity $1_D^{(sys)}$. Assuming $N_{z,D} \gg 1$ (equivalent to $N_D \gg N_{xy,D}$), we have

$$\gamma_{A\leftarrow dark_D} = \frac{2\pi}{\hbar}\frac{1}{N_D}\sum_l\sum_{i,j}|\langle A_{l0}|H_{DA}|D_{ij}\rangle|^2 J_{A,D} - \frac{2\pi}{\hbar}\frac{1}{N_D}\sum_l\sum_{\vec{k}\in\text{FBZ}}|\langle A_{l0}|H_{DA}|D_{\vec{k}}\rangle|^2 J_{A,D}. \tag{S25}$$

We note that the first term is exactly $\gamma_{\text{bare FRET}}$. Applying the arguments from the derivation (Section S2.4, including the orientational averaging approximations of Eqs. (S21) and (S22)) of the rate of EET from donor polaritons to acceptors, as well as the continuum approximation, we obtain

$$\gamma_{A\leftarrow dark_D} = \frac{2\pi}{\hbar}\rho_A^{(2D)}\mu_D^2\mu_A^2\langle\kappa_{FRET}^2\rangle\left[\frac{\int_s^{s+\mathscr{W}} dz\frac{\pi}{2(z_{0,A}-z)^4}}{\mathscr{W}} - \frac{1}{N_D}\sum_{\vec{k}\in\text{FBZ}}\frac{\int_s^{s+\mathscr{W}} dz e^{-2a_{d\vec{k}}z}\frac{\pi}{2(z_{0,A}-z)^4}}{\int_s^{s+\mathscr{W}} dz e^{-2a_{d\vec{k}}z}}\right] J_{AD}. \tag{S26}$$

Using $\sum_{\vec{k}\in\text{FBZ}} = N_{xy,D}$ and $N_{z,D} \gg 1$, we arrive at

$$\begin{aligned}\frac{1}{N_D}\sum_{\vec{k}\in\text{FBZ}}\frac{\int_s^{s+\mathscr{W}} dz e^{-2a_{d\vec{k}}z}\frac{\pi}{2(z_{0,A}-z)^4}}{\int_s^{s+\mathscr{W}} dz e^{-2a_{d\vec{k}}z}} &\le \frac{1}{N_{z,D}}\max_{\vec{k}\in\text{FBZ}}\frac{\int_s^{s+\mathscr{W}} dz e^{-2a_{d\vec{k}}z}\frac{\pi}{2(z_{0,A}-z)^4}}{\int_s^{s+\mathscr{W}} dz e^{-2a_{d\vec{k}}z}} \\ &\ll \frac{\int_s^{s+\mathscr{W}} dz\frac{\pi}{2(z_{0,A}-z)^4}}{\mathscr{W}},\end{aligned} \tag{S27}$$

which yields

$$\gamma_{A\leftarrow dark_D} \approx \frac{2\pi}{\hbar}\rho_A^{(2D)}\mu_D^2\mu_A^2\langle\kappa_{FRET}^2\rangle\frac{\frac{\pi}{6}\left[\frac{1}{(z_{0,A}-s-\mathscr{W})^3} - \frac{1}{(z_{0,A}-s)^3}\right]}{\mathscr{W}} J_{AD}. \tag{S28}$$

This expression is exactly the bare FRET rate $\gamma_{\text{bare FRET}}$ of Eq. (13b) under the aforementioned assumptions of infinitely extended slab along the xy plane, translational symmetry, orientational averaging, and the continuum limit.

S2.6 Additional simulation notes/data for donors SC

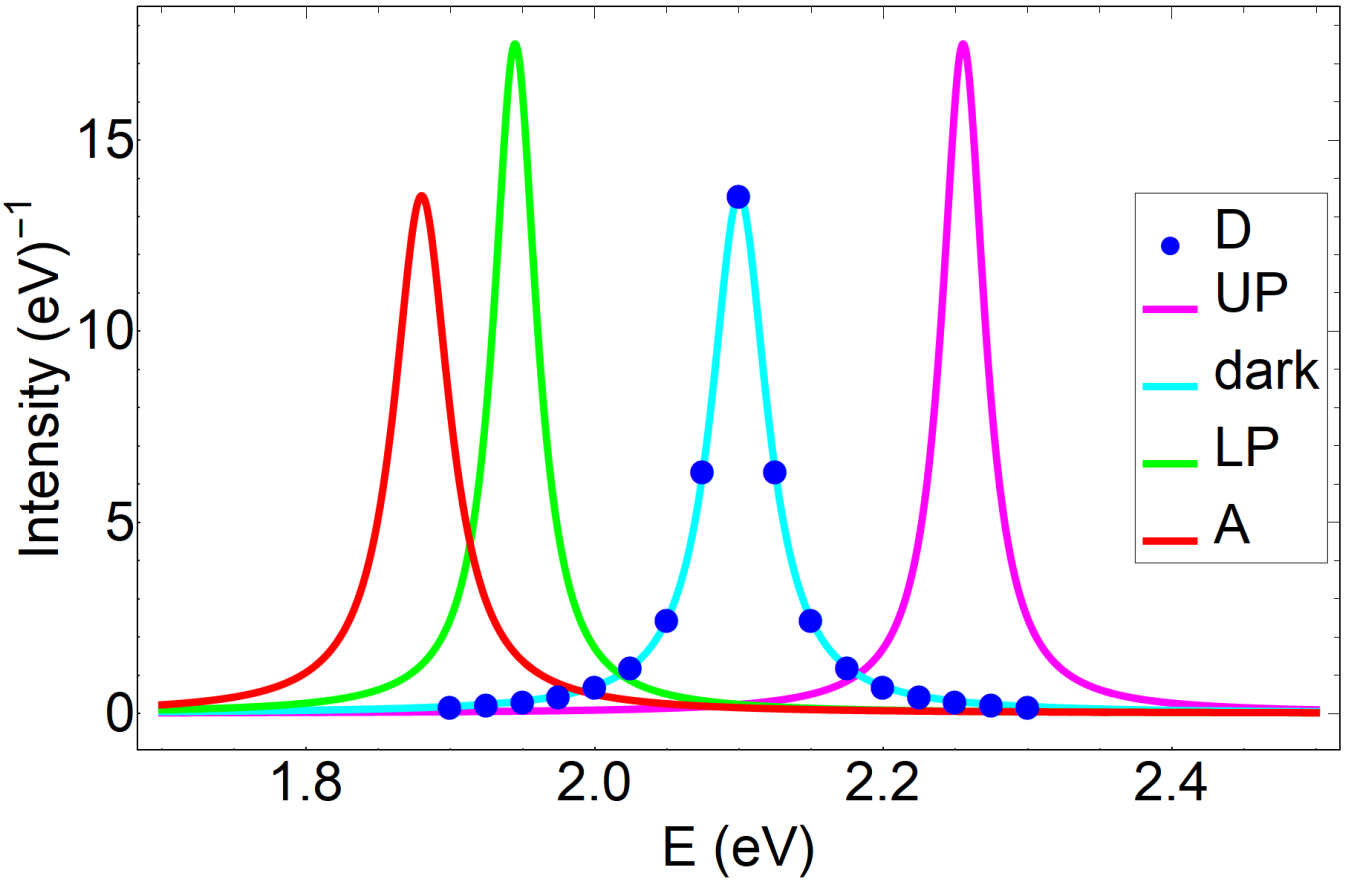

Fig. S1 SC of SPs to donors. Lorentzian spectra for the donor polariton and dark states (formed with donor-resonant SP mode), as well as the bare donors and acceptors.

S2.7 Derivation of simulated rates for acceptors SC

The simulated rates for EET from a monolayer of bare donor at $z = z_{0,D} > z_{m,A}$ for all m to acceptor polariton/dark states asssuming a thick acceptor slab ($N_A \gg N_{xy,A}$), orientational averaging and no correlations for the TDMs $\vec{\mu}_{A_{lm}}$ are given by

$$\gamma_{\alpha_A \leftarrow D} = \frac{1}{\hbar}\int_0^{\pi/a} dk\, k \left[|c_{A_{\vec{k}}\alpha_{A,\vec{k}}}|^2 \mu_D^2 \mu_A^2 \langle \kappa_{FRET}^2 \rangle \frac{\int_s^{s+\mathscr{W}} dz e^{-2a_{d\vec{k}}z} \frac{\pi}{2(z_{0,D}-z)^4}}{\frac{e^{-2a_{d\vec{k}}(s+\mathscr{W})} - e^{-2a_{d\vec{k}}s}}{-2\alpha_{d\vec{k}}}} + |c_{\vec{k}\alpha_{A,\vec{k}}}|^2 \mu_D^2 \langle |\kappa_{LM,\vec{k}}|^2 \rangle \frac{\hbar\omega_{\vec{k}}}{2\varepsilon_0 L_{\vec{k}}} e^{-2a_{d\vec{k}}z_{0,D}} \right] J_{\alpha_{A,\vec{k}}D} \tag{S29a}$$

$$\gamma_{dark_A \leftarrow D} = \frac{2\pi}{\hbar}\rho_A \mu_D^2 \mu_A^2 \langle \kappa_{FRET}^2 \rangle \frac{\pi}{6}\left[\frac{1}{(z_{0,D}-s-\mathscr{W})^3} - \frac{1}{(z_{0,D}-s)^3} \right] J_{AD} = \gamma'_{\text{bare FRET}}, \tag{S29b}$$

where $\gamma'_{\text{bare FRET}}$ is the bare FRET rate. Here, the thickness of the acceptor slab is $\mathscr{W}$, its base is located at $z = s$, and its (three-dimensional) concentration is $\rho_A = \frac{N_A}{S\mathscr{W}}$. The derivation of Eq. (S29) starts with the preliminary rate expression in Eq. (9) of the main text and proceeds analogously to those in Sections S2.4 and S2.5, respectively. In contrast to Eq. (S23), Eq. (S29a) also sums over the final polariton $\vec{k}$ modes, yielding a integral rate upon invoking the continuum-limit transformation $\sum_{\vec{k}\in\text{FBZ}} \rightarrow \frac{S}{(2\pi)^2}\int_0^{2\pi} d\phi \int_0^{\pi/a} dk\, k$ for acceptor lattice spacing a. Eq. (S29) is a more explicit form of Eq. 13 in the main text.

We now consider the case when

$$\frac{1}{N_{xy,A}} \sum_{\vec{k}\in\text{FBZ}} |\langle \vec{k}|H_{DP}|D_{i0}\rangle|^2 < \frac{1}{N_A}\sum_{l,m} |\langle A_{lm}|H_{DA}|D_{i0}\rangle|^2, \tag{S30}$$

in other words, the average PRET coupling intensity is smaller than that of FRET; this can happen when the donor-acceptor separation lies within the typical FRET range (1-10 nm). As we next show, the EET rate from a monolayer of bare donors to acceptor polariton band α_A is consequently much smaller than the bare FRET rate ($\gamma'_{\text{bare FRET}}$ in Eq. (13b)) as $N_A \gg N_{xy,A}$ (*i.e.*, $N_{z,A} \gg 1$), for isotropic and uncorrelated orientational distribution of TDMs $\vec{\mu}_{A_{lm}}, \vec{\mu}_{D_{i0}}$. The steps taken here resemble those employed in Section S2.5. Starting from Eq. (13a), we utilize $|c_{A_{lm}A_{\vec{k}}}|^2 \approx \frac{1}{N_A}$ to obtain

$$\begin{aligned}
\gamma_{\alpha_A \leftarrow D} &\approx \frac{2\pi}{\hbar N_D} \sum_{\vec{k}\in\text{FBZ}} \sum_i \left[|c_{A_{\vec{k}}\alpha_{A,\vec{k}}}|^2 \sum_{l,m} \frac{1}{N_A} |\langle A_{lm}|H_{DA}|D_{i0}\rangle|^2 + |c_{\vec{k}\alpha_{A,\vec{k}}}|^2 |\langle \vec{k}|H_{DP}|D_{i0}\rangle|^2 \right] J_{\alpha_{A,\vec{k}},D} \\
&\leq \frac{2\pi}{\hbar N_D} \sum_i \sum_{l,m} |\langle A_{lm}|H_{DA}|D_{i0}\rangle|^2 \frac{1}{N_{z,A}} \max_{\vec{k}\in\text{FBZ}} J_{\alpha_{A,\vec{k}},D} \\
&\quad + \frac{2\pi}{\hbar N_D} \sum_i \sum_{\vec{k}\in\text{FBZ}} |\langle \vec{k}|H_{DP}|D_{i0}\rangle|^2 \max_{\vec{k}\in\text{FBZ}} J_{\alpha_{A,\vec{k}},D} \\
&\ll \frac{2\pi}{\hbar N_D} \sum_i \sum_{l,m} |\langle A_{lm}|H_{DA}|D_{i0}\rangle|^2 J_{A,D} \\
&= \gamma'_{\text{bare FRET}},
\end{aligned} \tag{S31}$$

where the second inequality holds for sufficiently large $N_{z,A}$ such that $\frac{2}{N_{z,A}} \max_{\vec{k}\in\text{FBZ}} J_{\alpha_{A,\vec{k}},D} \ll J_{A,D}$. This result can be physically interpreted as follows: $\gamma'_{\text{bare FRET}}$ and $\gamma^{FRET}_{\alpha_A \leftarrow D}$ scale as the number of final states N_A and $N_{xy,A} \ll N_A$, respectively.

S2.8 Additional simulation notes/data for acceptors SC

We note that the rates from donors to polariton bands (Eq. S29a) were calculated numerically. In particular, the integrals over k were calculated via the trapezoidal rule using 2000 intervals.

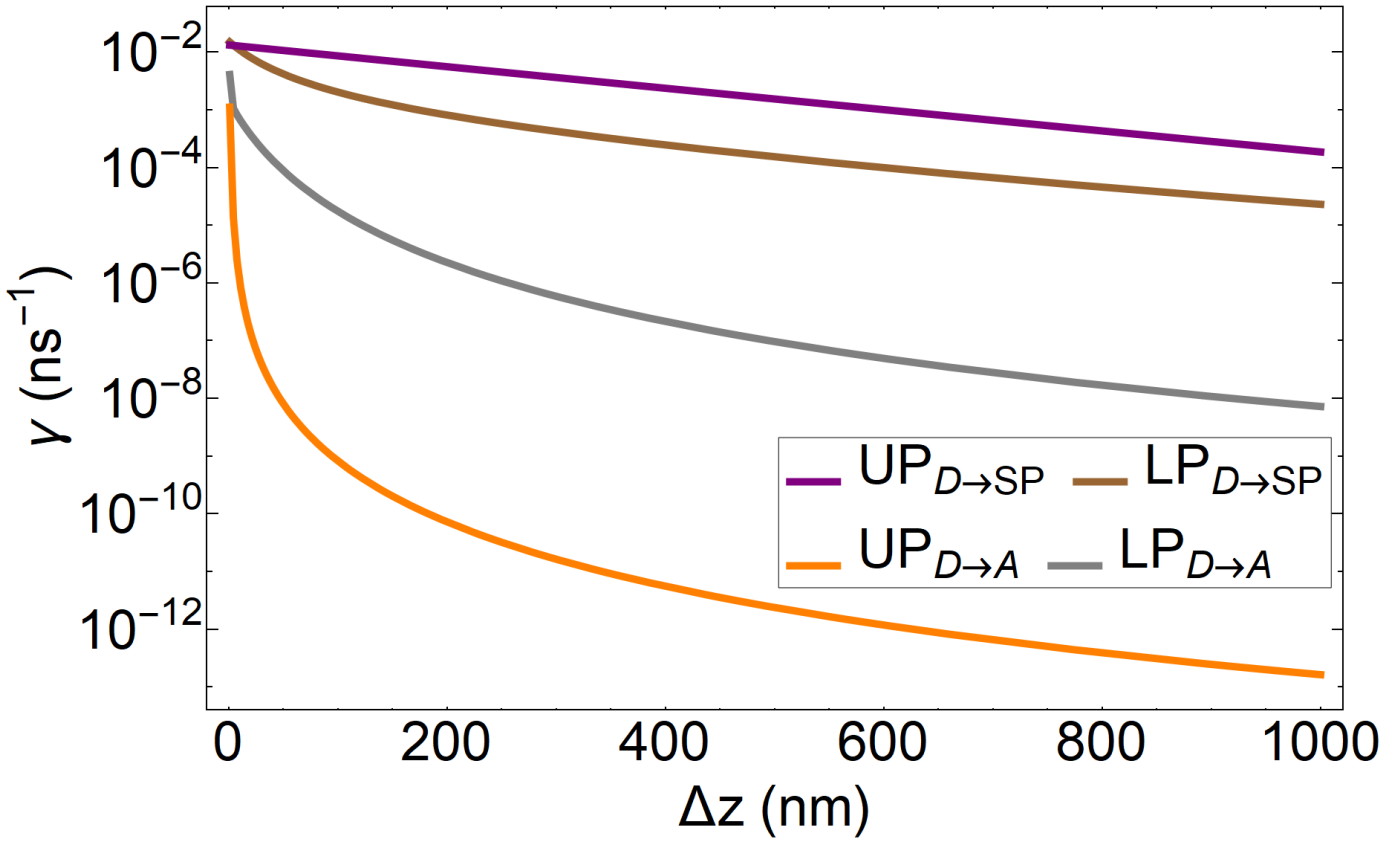

Fig. S2 SC of SPs to acceptors. Contributions of EET rates from donors to acceptor UP and LP due to donor-acceptor (FRET) and SP-donor (PRET) interactions.

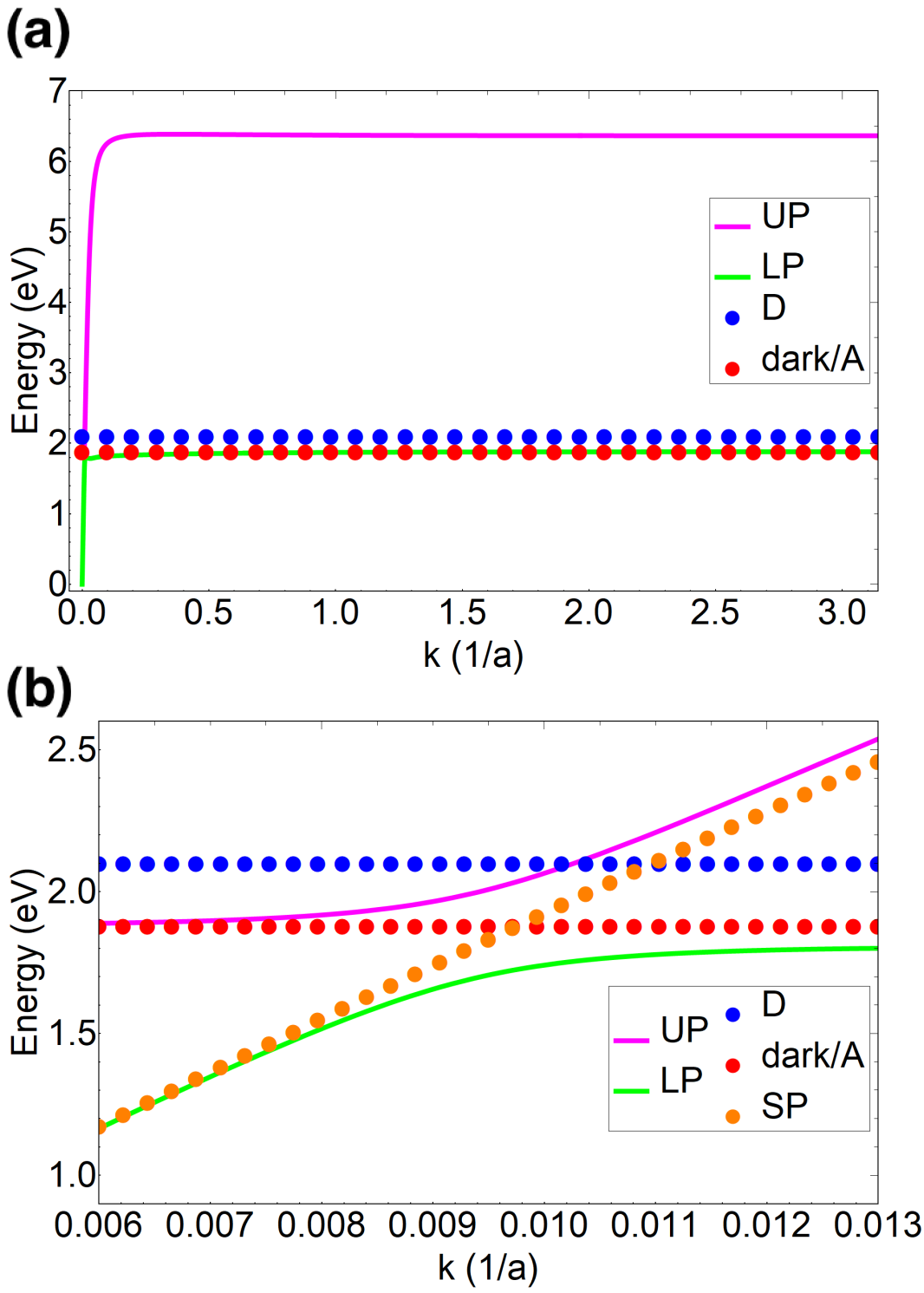

Fig. S3 SC of SPs to acceptors.(a) Dispersion curve in the FBZ. The value $a = 1 \times 10^{-9}$ m is the inter-chromophoric lattice spacing for the acceptor slab. (b) Expanded view of dispersion curve at region of anticrossing characteristic of SC; the SP dispersion has been added to help visualize the anticrossing.

S2.9 Simulations for the "carnival effect"

For this simulation, the coupling is strong enough such that the UP is higher in energy than the bare donors. Thus, the acceptor UP becomes a donor and the donors turn into acceptors. We use the rate Eq. (S23) derived for the case of exclusive donor SC for transfer from a polariton state with the labels D and A interchanged.

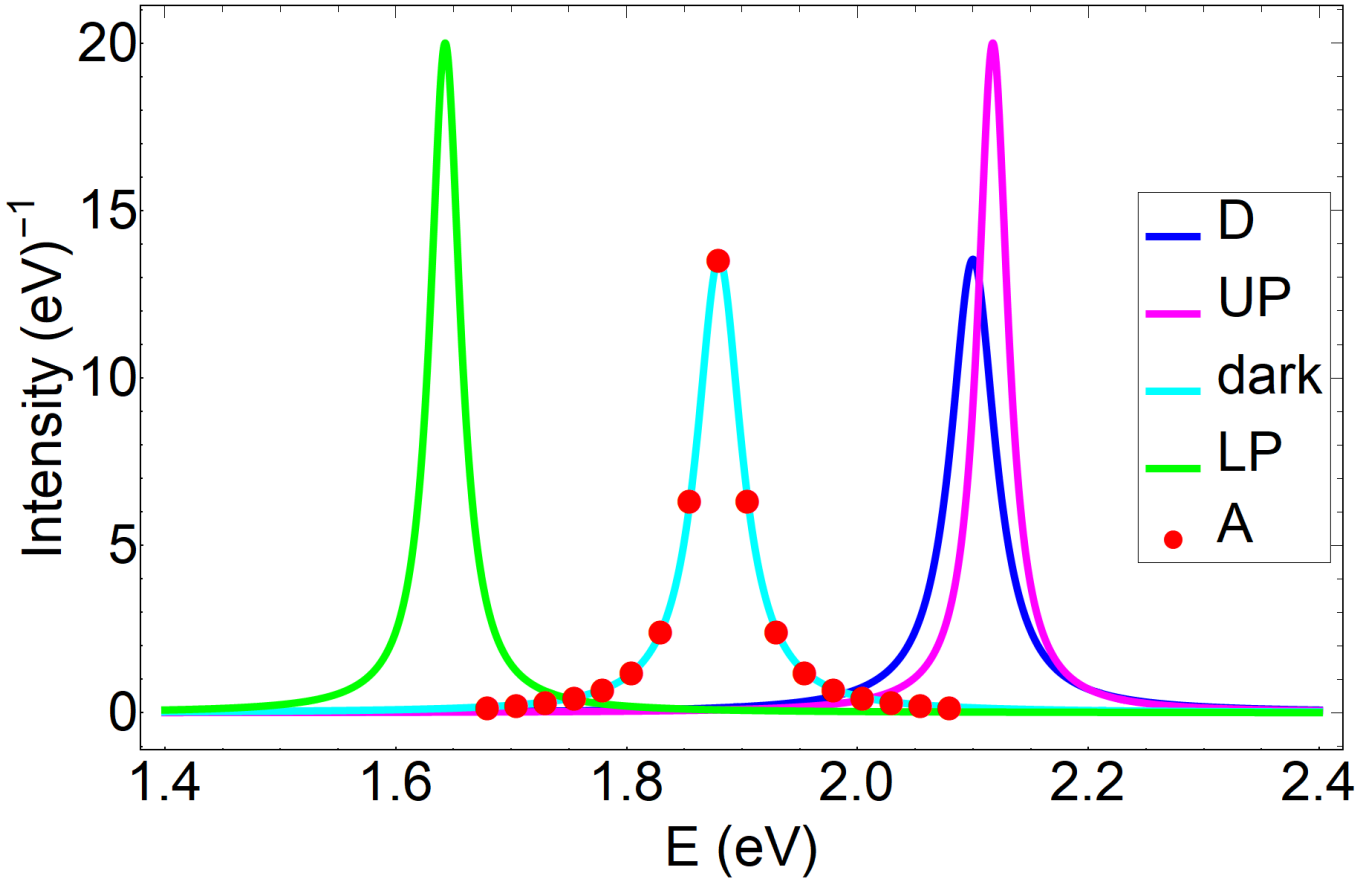

Fig. S4 Carnival effect of EET role-reversal. Lorentzian spectra for the acceptor polariton and dark states (formed with acceptor-resonant SP mode), as well as the bare donors and acceptors.

S3 Case *ii*

S3.1 Derivation: EET rates Eq. (11)

In this section, we show how to derive the EET rates in Eq. (11) of the main text between polariton/dark states when both donors and acceptors are strongly coupled to SP modes. While we only derive rate Eq. (11a) in significant detail, Eqs. (11b) and (11c) can be analogously obtained in essentially the same manner.

Excitons coupled to the $\vec{k}$-th SP mode produce polariton states of the form $|\alpha_{\vec{k}}\rangle = c_{D_{\vec{k}}\alpha_{\vec{k}}}|D_{\vec{k}}\rangle + c_{A_{\vec{k}}\alpha_{\vec{k}}}|A_{\vec{k}}\rangle + c_{\vec{k}\alpha_{\vec{k}}}|\vec{k}\rangle$. As discussed in the main text, for sufficiently large separation between donor and acceptor slabs, the perturbation $V^{(ii)}$ due to the chromophore and photon baths induces transitions between the UP, MP, LP and dark states of donors and acceptors:

$$V^{(ii)} = \sum_C \sum_{i,j} |C_{ij}\rangle\langle C_{ij}| \sum_q \lambda_{q,C}\hbar\omega_{q,C}(b^\dagger_{q,C_{ij}} + \text{h.c.}) + \sum_{\vec{k}}\sum_q g_{q,\vec{k}}(b^\dagger_{q,P}a_{\vec{k}} + \text{h.c.}), \tag{S32}$$

where $C = D,A$. Neglect of H_{DA} in $V^{(ii)}$ is justified by FRET decaying with increasing interslab distance and occurring slower than vibrational relaxation in typical organic molecules.[S17] Given the locality of vibronic coupling, the first term only couples two states that share the same chromophores. On the other hand, the second term does not couple different polariton/dark states because it represents radiative and Ohmic losses from the SP modes. The EET rate from a single polariton state $|\alpha_{\vec{k}}\rangle$ to the polariton band β can then be calculated by invoking FGR,

$$\begin{aligned}\gamma_{\beta\leftarrow\alpha_{\vec{k}}} = &\sum_{\vec{k}'\in\text{FBZ}}\sum_C |c_{C_{\vec{k}'}\beta_{\vec{k}'}}|^2|c_{C_{\vec{k}}\alpha_{\vec{k}}}|^2\sum_{i,j}|c_{C_{ij}C_{\vec{k}'}}|^2|c_{C_{ij}C_{\vec{k}}}|^2 \\ &\times\frac{2\pi}{\hbar^2}\sum_{L'}\sum_L p_{L_{C_{ij}}}|\langle L'_{C_{ij}}|\sum_q\lambda_{q,C}\hbar\omega_{q,C}(b^\dagger_{q,C_{ij}}+b_{q,C_{ij}})|L_{C_{ij}}\rangle|^2\delta(\omega_{\beta_{\vec{k}'}\alpha_{\vec{k}}}+\omega_{L'_{C_{ij}}L_{C_{ij}}}).\end{aligned} \tag{S33}$$

$|L_{C_{ij}}\rangle$ refers to a local bath state of molecule C_{ij} and $p_{L_{C_{ij}}}$ is the thermal probability to populate it. Assuming that all molecules of the same type C (donor or acceptor) feature the same bath modes, we can associate the single-molecule rate

$$\frac{2\pi}{\hbar^2}\sum_{L'}\sum_L p_{L_{C_{ij}}}|\langle L'_{C_{ij}}|\sum_q\lambda_{q,C}\hbar\omega_{q,C}(b^\dagger_{q,C_{ij}}+b_{q,C_{ij}})|L_{C_{ij}}\rangle|^2\delta(\omega+\omega_{L'_{C_{ij}}L_{C_{ij}}}) = \mathscr{R}_C(\omega) \tag{S34}$$

which can be readily related to a spectral density, as explained in the main text. Then we arrive at the compact expression,

$$\gamma_{\beta\leftarrow\alpha_{\vec{k}}} = \sum_{\vec{k}'\in\text{FBZ}}\sum_C |c_{C_{\vec{k}'}\beta_{\vec{k}'}}|^2|c_{C_{\vec{k}}\alpha_{\vec{k}}}|^2\sum_{i,j}|c_{C_{ij}C_{\vec{k}'}}|^2|c_{C_{ij}C_{\vec{k}}}|^2\mathscr{R}_C(\omega_{\beta_{\vec{k}'}\alpha_{\vec{k}}}), \tag{S35}$$

which is exactly Eq. (11a) of the main text.

To derive the average rate Eq. (11b) from dark states of chromophore C to the polariton band α, we begin with

$$\gamma_{\alpha\leftarrow dark_C} = \frac{2\pi}{\hbar^2}\sum_{\vec{k}'\in\text{FBZ}}\frac{1}{N_C - N_{xy,C}}\sum_{\vec{k}\in\text{FBZ}}\sum_d\sum_{i'j'}\sum_{L'}\sum_{i''j''}\sum_L p_{L_{C_{i''j''}}}|\langle\alpha_{\vec{k}'}, L'_{C_{i'j'}}|V^{(ii)}|d_{C,\vec{k}}, L_{C_{i''j''}}\rangle|^2\delta(\omega_{\alpha_{\vec{k}'}C}+\omega_{L'_{C_{i'j'}}L_{C_{i''j''}}}). \tag{S36}$$

Similarly, the derivation of rate Eq. (11c) from polariton state $|\alpha_{\vec{k}}\rangle$ to the same dark states starts at

$$\gamma_{dark_C\leftarrow\alpha_{\vec{k}}} = \frac{2\pi}{\hbar^2}\sum_{\vec{k}\in\text{FBZ}}\sum_d\sum_{i'j'}\sum_{L'}\sum_{i''j''}\sum_L p_{L_{C_{i''j''}}}|\langle d_{C,\vec{k}'}, L'_{C_{i'j'}}|V^{(ii)}|\alpha_{\vec{k}}, L_{C_{i''j''}}\rangle|^2\delta(\omega_{C\alpha_{\vec{k}}}+\omega_{L'_{C_{i'j'}}L_{C_{i''j''}}}). \tag{S37}$$

We note that the presence of the prefactor $\frac{1}{N_C-N_{xy,C}}$ in Eq. (S36) and lack thereof in Eq. (S37) is due to the asymmetry of FGR: in the former equation, dark states serve as the initial state and thus the term for each state is weighted by its occupation probability, which we have assumed to be uniform at $\frac{1}{N_C-N_{xy,C}}$ given their degeneracy.

S3.2 Simulated rates

In this section, we present the rates used in our simulations for both donors and acceptors strongly coupled to SPs assuming (as discussed in the main text) orientationally averaged TDMs $\vec{\mu}_{C_{ij}}$, $N_{xy,D} = N_{xy,A} = N_{xy}$, and $N_{z,C} \gg 1$ for $C = D,A$.

The overlap between $|C_{ij}\rangle$ and the collective mode $|C_{\vec{k}}\rangle$ can be written as $|c_{C_{ij}C_{\vec{k}}}| = \frac{\kappa_{\vec{k}C_{ij}}e^{-a_{d\vec{k}}z_{j,C}}}{\sqrt{\sum_{i,j}|\kappa_{\vec{k}C_{ij}}|^2e^{-2a_{d\vec{k}}z_{j,C}}}}$ and plugged into Eq. (11a) to

obtain the rate for EET from polariton state $|\alpha_{\vec{k}}\rangle$ to band β:

$$\gamma_{\beta\leftarrow\alpha_{\vec{k}}} = \frac{1}{2\pi}\sum_C \frac{|c_{C_{\vec{k}}\alpha}|^2}{\rho_C \frac{e^{-2a_{d\vec{k}}(s_C+\mathscr{W}_C)}-e^{-2a_{d\vec{k}}s_C}}{-2a_{d\vec{k}}}} \int_0^{\pi/a} dk'\, k' |c_{C_{\vec{k}}\beta}|^2 \frac{\frac{e^{-2(a_{d\vec{k}}+a_{d\vec{k}'})(s_D+\mathscr{W}_D)}-e^{-2(a_{d\vec{k}}+a_{d\vec{k}'})s_D}}{-4a_{d\vec{k}'}}}{\frac{e^{-2a_{d\vec{k}'}(s_D+\mathscr{W}_D)}-e^{-2a_{d\vec{k}'}s_D}}{-2a_{d\vec{k}'}}} \mathscr{R}_D(\omega_{\beta_{\vec{k}'}\alpha_{\vec{k}}}), \tag{S38}$$

where we have applied orientational averaging of the TDMs under the approximation $\langle |c_{C_{ij}C_{\vec{k}}}|^2\rangle \approx \frac{e^{-2a_{d\vec{k}}z_{j,C}}}{N_{xy}\sum_j e^{-2a_{d\vec{k}}z_{j,C}}}$ (Section S2.4) and the $\vec{k}$-space continuum-limit transformation (Section S2.7).

The derivation of the EET rate from polariton $|\alpha_{\vec{k}}\rangle$ to dark states is quite alike that of Section S2.5. We can write Eq. (11c) as

$$\gamma_{dark_C\leftarrow\alpha_{\vec{k}}} = |c_{C_{\vec{k}}\alpha_{\vec{k}}}|^2 \mathscr{R}_C(\omega_{C\alpha_{\vec{k}}}) \sum_{i,j} |c_{C_{ij}C_{\vec{k}}}|^2 \sum_{\vec{k}'\in \mathrm{FBZ}} \sum_d |\langle C_{ij}|d_{C,\vec{k}'}\rangle|^2. \tag{S39}$$

Inserting the relation $\sum_{\vec{k}\in\mathrm{FBZ}}\sum_d |d_{C,\vec{k}}\rangle\langle d_{C,\vec{k}}| = 1_C^{(sys)} - \sum_{\vec{k}\in\mathrm{FBZ}} |C_{\vec{k}}\rangle\langle C_{\vec{k}}|$, we obtain

$$\gamma_{dark_C\leftarrow\alpha_{\vec{k}}} = |c_{C_{\vec{k}}\alpha_{\vec{k}}}|^2 \mathscr{R}_C(\omega_{C\alpha_{\vec{k}}}) \sum_{i,j} |c_{C_{ij}C_{\vec{k}}}|^2 \left(1 - \sum_{\vec{k}'\in\mathrm{FBZ}} |c_{C_{ij}C_{\vec{k}'}}|^2\right). \tag{S40}$$

Noting that $|c_{C_{ij}C_{\vec{k}'}}|^2 \sim \frac{1}{N_{xy}N_{z,C}}$ and $\sum_{\vec{k}\in\mathrm{FBZ}}$ sums over N_{xy} terms, we utilize $N_{z,C}\gg 1$ and $\sum_{i,j}|c_{C_{ij}C_{\vec{k}}}|^2 = 1$ to write

$$\gamma_{dark_C\leftarrow\alpha_{\vec{k}}} = |c_{C_{\vec{k}}\alpha_{\vec{k}}}|^2 \mathscr{R}_C(\omega_{C\alpha_{\vec{k}}}). \tag{S41}$$

This same logic can be applied to arrive at

$$\gamma_{\alpha\leftarrow dark_C} = \frac{1}{2\pi\rho_C\mathscr{W}_C}\int_0^{\pi/a} dk'\, k' |c_{C_{\vec{k}'}\alpha_{\vec{k}'}}|^2 \mathscr{R}_C(\omega_{\alpha_{\vec{k}'}C}) \tag{S42}$$

for a continuum of $\vec{k}$ states.

In summary, the simulated equations for the case where both donors and acceptors are strongly coupled are

$$\gamma_{\beta\leftarrow\alpha_{\vec{k}}} = \frac{1}{2\pi}\sum_C \frac{|c_{C_{\vec{k}}\alpha}|^2}{\rho_C \frac{e^{-2a_{d\vec{k}}(s_C+\mathscr{W}_C)}-e^{-2a_{d\vec{k}}s_C}}{-2a_{d\vec{k}}}} \int_0^{\pi/a} dk'\, k' |c_{C_{\vec{k}}\beta}|^2 \frac{\frac{e^{-2(a_{d\vec{k}}+a_{d\vec{k}'})(s_D+\mathscr{W}_D)}-e^{-2(a_{d\vec{k}}+a_{d\vec{k}'})s_D}}{-4a_{d\vec{k}'}}}{\frac{e^{-2a_{d\vec{k}'}(s_D+\mathscr{W}_D)}-e^{-2a_{d\vec{k}'}s_D}}{-2a_{d\vec{k}'}}} \mathscr{R}_D(\omega_{\beta_{\vec{k}'}\alpha_{\vec{k}}}), \tag{S43a}$$

$$\gamma_{\alpha\leftarrow dark_C} = \frac{1}{2\pi\rho_C\mathscr{W}_C}\int_0^{\pi/a} dk'\, k' |c_{C_{\vec{k}'}\alpha_{\vec{k}'}}|^2 \mathscr{R}_C(\omega_{\alpha_{\vec{k}'}C}), \tag{S43b}$$

$$\gamma_{dark_C\leftarrow\alpha_{\vec{k}}} = |c_{C_{\vec{k}}\alpha_{\vec{k}}}|^2 \mathscr{R}_C(\omega_{C\alpha_{\vec{k}}}). \tag{S43c}$$

From these expressions, it can be seen that the rates to polariton bands (Eqs. (S43a) and (S43b)) scale as $\sim \frac{1}{N_{z,C}}$ relative to the rate to dark states (Eq. (S43c)), which scales as a single-molecule rate $\mathscr{R}_C$. This is because there are N_{xy} states in each polariton band as opposed to $N_C - N_{xy}$ in the band of dark states.

As discussed in the main text (Section 3), the spectral density that governs $\mathscr{R}_C(\omega)$ depends on the energies $\hbar\omega_q$ and coupling strengths $\lambda_q\hbar\omega_q$ of representative localized vibrational modes B_{TDBC}, reproduced below from literature:[S18]

$\hbar\omega_q$ (meV)	40	80	120	150	185	197
$\lambda_q\hbar\omega_q$ (meV)	14	18	25	43	42	67

S3.3 Rate parameters for comparison to experiments

Here, we present closed-form expressions for certain rate parameters characterizing downhill vibrational-relaxation transitions between polariton and dark states. Specifically, these rate parameters were first introduced as empirical constants fitted to the data of Coles et al.[S19] For spatially separated slabs of donors and acceptors—the setup studied in our work—such experimental values are not available in the literature. Instead, we compare to those of Coles et al. for a blend of donors and acceptors. This comparison is supported by qualitatively similar photoluminescence for both setups, as reported by the same authors.[S19]

Based on their fitting model (Eqs. (3)-(5) of Ref.[S19]), we express their rate parameters $\{\mathscr{C}_5^{\mathrm{UPB}} = (34\text{ fs})^{-1}, \mathscr{C}_2 = (603\text{ ps})^{-1}, \mathscr{C}_5^{\mathrm{MPB}} = (8.5\text{ fs})^{-1}, \mathscr{C}_1 = (228\text{ ps})^{-1}\}$ (Table 1 of Ref.[S19]) in terms of our theoretical framework as follows (throughout this section we use the

convention $c_{a,b} = \langle a|b\rangle$ and $\omega_{f,i} = \omega_f - \omega_i$):

$$\mathscr{C}_5^{\mathrm{UPB}} \equiv \max_{\vec{k}}\{\gamma_{dark_D \leftarrow \mathrm{UP}_{\vec{k}}}\}, \tag{S44a}$$

$$\mathscr{C}_2 \equiv N_{dark_D}\left\langle 2\pi\, \mathscr{J}_D(-\omega_{\mathrm{MP}_{\vec{k}},D})\frac{\pi k^2}{(2\pi)^2/S}\frac{1}{N_D}\right\rangle_{\vec{k}} \tag{S44b}$$

$$= \frac{N_{dark_D}}{2\rho_D \mathscr{W}_D}\frac{\int_{k_{\min}}^{k_{\max}} dk'\,(k')^3\,\mathscr{J}_D(-\omega_{\mathrm{MP}_{\vec{k}'},D})}{\frac{1}{2}(k_{\max}^2 - k_{\min}^2)}, \tag{S44c}$$

$$\mathscr{C}_5^{\mathrm{MPB}} \equiv \max_{\vec{k}}\{\gamma_{dark_A \leftarrow \mathrm{MP}_{\vec{k}}}\}, \tag{S44d}$$

$$\mathscr{C}_1 \equiv N_{dark_A}\left\langle 2\pi\, \mathscr{J}_A(\omega_{-\mathrm{LP}_{\vec{k}},A})\frac{\pi k^2}{(2\pi)^2/S}\frac{1}{N_A}\right\rangle_{\vec{k}} \tag{S44e}$$

$$= \frac{N_{dark_A}}{2\rho_A \mathscr{W}_A}\frac{\int_{k_{\min}}^{k_{\max}} dk'\,(k')^3\,\mathscr{J}_A(-\omega_{\mathrm{LP}_{\vec{k}'},A})}{\frac{1}{2}(k_{\max}^2 - k_{\min}^2)}, \tag{S44f}$$

where the relations in Eqs. (S44b) and (S44e) were obtained by comparing the first terms on the right-hand sides of Eqs. (4) and (3) of Ref.[S19], respectively, with Eq. (15) of the theoretical work by Michetti and La Rocca.[S20] The particular $k_{\min}, k_{\max}$ used in calculation of $\mathscr{C}_2$ and $\mathscr{C}_1$ in Table 2 of the main text are given in the next section. $\mathscr{J}_C(\omega)$ is the spectral density (defined after Eq. (11) of the main text) for chromophore $C = D, A$. N_{dark_C} is a fitting constant proportional to the steady-state population—assumed to be independent of the wavevector by Coles et al. Notice that $\mathscr{C}_5^{\mathrm{UPB}}$ and $\mathscr{C}_5^{\mathrm{MPB}}$ can be numerically evaluated using theory presented above (Eq. S43c). However, numerical computation of $\mathscr{C}_2$ and $\mathscr{C}_1$ requires the values of N_{dark_C}, which are not actually defined by Coles et al.[S19] Given that Coles et al. determined $\mathscr{C}_2$ and $\mathscr{C}_1$ partly by using the work of Michetti and La Rocca[S20] (see first four sentences of footnotes of Table 1 in Ref.[S19]), we next estimate N_{dark_C} using experimental results from Ref.[S19] and the theoretical results from[S20].

The first step is to relate $\mathscr{C}_2$ and $\mathscr{C}_1$ to FGR rates $\gamma_{\mathrm{MP}_{\vec{k}} \leftarrow dark_D}$ and $\gamma_{\mathrm{LP}_{\vec{k}} \leftarrow dark_A}$ (Eq. (S43b)) using Eqs. (4) and (3), respectively, of Ref.[S19]:[S21]

$$N_{dark_D} \approx \frac{(603\text{ ps})^{-1}\left\langle |c_{D,\mathrm{MP}_\theta}|^2[n(-\omega_{\mathrm{MP}_\theta,D})+1]\right\rangle_\theta}{\langle \gamma_{\mathrm{MP}_\theta \leftarrow dark_D}\rangle_\theta}, \tag{S45a}$$

$$N_{dark_A} \approx \frac{(228\text{ ps})^{-1}\left\langle |c_{A,\mathrm{LP}_\theta}|^2[n(-\omega_{\mathrm{LP}_\theta,A})+1]\left(\frac{|\omega_{\mathrm{LP}_\theta,A}|}{75\text{ meV}/\hbar}\right)^{1.93}\right\rangle_\theta}{\langle \gamma_{\mathrm{LP}_\theta \leftarrow dark_A}\rangle_\theta}, \tag{S45b}$$

where $|c_{C,\alpha_\theta}|^2$ is the fraction of exciton C in polariton state α_θ for $(C,\alpha) = (D,\mathrm{MP}), (A,\mathrm{LP})$ and $n(\omega) = \frac{1}{e^{\hbar\omega/k_BT}-1}$ is the Bose-Einstein distribution function. We have replaced $\vec{k}$ with θ to indicate quantities that are either experimentally determined for a polariton state excited by a laser with this incident angle (see Coles et al.[S19] for further experimental details) or estimated from Michetti and La Rocca[S20]. We carry out the averages $\langle\cdot\rangle_\theta$ above over the θ-interval $[\theta_{\min} = 17^\circ, \theta_{\max} = 56^\circ]$ by approximate fitting of the data of Coles et al.[S19] as follows:

- $$|c_{D,\mathrm{MP}_\theta}|^2 = \begin{cases} 0 & \theta \in [\theta_{\min}, 27^\circ] \\ \frac{0.8}{\theta_{\max}-27^\circ}(\theta - \theta_{\max}) + 0.8 & \theta \in [27^\circ, \theta_{\max}] \end{cases} \tag{S46}$$

  (Fig. 3d of Coles et al.[S19])

- $n(-\omega_{\mathrm{MP}_\theta,D}) \approx 0$ because $|\omega_{\mathrm{MP}_\theta,D}| \gg k_BT$ (Figs. 4a-4c of Coles et al.[S19])

- $$|c_{A,\mathrm{LP}_\theta}|^2 = \begin{cases} \frac{0.9}{47^\circ-\theta_{\min}}(\theta - 47^\circ) + 0.9 & \theta \in [\theta_{\min}, 47^\circ] \\ 0.9 & \theta \in [47^\circ, \theta_{\max}] \end{cases} \tag{S47}$$

  (Fig. 3e of Coles et al.[S19]),

- $$\omega_{\mathrm{LP}_\theta,A}(\mathrm{nm}^{-1}) = \frac{1}{\frac{-30\text{ nm}}{\theta_{\max}-\theta_{\min}}(\theta - \theta_{\max}) + 640\text{ nm}} - \frac{1}{636.4\text{ nm}} \tag{S48}$$

(Figs. 4a-4c of Coles et al.[S19]),

- $\langle \gamma_{\mathrm{MP}_\theta \leftarrow dark_D} \rangle_\theta \approx \langle \gamma_{\mathrm{LP}_\theta \leftarrow dark_A} \rangle_\theta \approx 10^7$ s^{-1} (roughly the average rate of scattering from the dark states to states in the LP close to the anticrossing for microcavity with a single strongly coupled J-aggregate cyanine dye, Fig. 6 of Michetti and La Rocca[S20]).

Then we arrive at $N_{dark_D} \approx 49$ and $N_{dark_A} \approx 112$.

Using these quantities, numerical values for Eq. (S44) can be calculated, as discussed in the next section. Comparison of the values to the rate parameters of Coles et al. is summarized in Table 2 of the main text.

S3.4 Additional simulation notes/data

We note that the rates in Eqs. (S43a) and (S43b) from polariton and dark states, respectively, to polariton bands were calculated numerically: as for the case of exclusive SC of acceptors to SPs (Section S2.8), the k-integrals were computed with the trapezoidal rule using 2000 intervals.

For the downhill energy transfer processes between polariton and dark states, we also compared (Table 2 of the main text) rate parameters $\mathscr{C}$ that were experimentally determined by Coles et al.[S19] to analogous theoretical rate parameters that we presented in the previous Section S3.3. The latter values, shown in the second column of Table 2, were calculated by computing the $\mathscr{C}$ in Eq. (S44)) with the same simulation conditions as for Fig. 4b, except considering $T = 300$ K and polariton k-interval $[k_{\min} = 0.8k_A, k_{\max} = 1.1k_D]$ (instead of $T = 0$ K and the entire FBZ, respectively; see next paragraph for justification). $k_A = 9.8 \times 10^6$ m^{-1} and $k_D = 1.1 \times 10^7$ m^{-1} are the anticrossing wavevectors for acceptors and donors, respectively. Given the reduced k-interval, the numerical integrals (Eqs. (S44c) and S44f) were evaluated using only 200 intervals (instead of 2000). The results are plotted in Fig. S7.

The above changes in temperature and k-interval were chosen to allow for a more direct comparison with the experiments of Coles et al. Their experiments were carried out at room temperature and only probed polariton states near the anticrossings. Our choice of $[k_{\min}, k_{\max}]$ comes from the paper of Hakala et al.[S22] To the best of our knowledge, this is the only work that studies a system with SPs strongly coupled to two organic-exciton bands and reports the concentration of the chromophore *after* it has been deposited on the metal and becomes strongly coupled to SPs. Specifically, the three polariton bands formed from hybridization of SPs and two exciton bands of Rhodamine 6G dye afforded absorption signal detectable in the window$\sim [1.2 \times 10^7$ m$^{-1}, 1.8 \times 10^7$ m$^{-1}]$, or between ~ 0.8 of the smaller anticrossing wavevector and ~ 1.1 of the bigger. This result stayed essentially the same for a wide range of concentrations, ranging from 0.1-10% of that used in this work for strongly coupled chromophores. So we employed $[k_{\min}, k_{\max}]$ for our calculation of $\mathscr{C}$ (without changing the concentration we assumed for Fig.4b).

It should be noted that between the systems of our work and Coles et al., there are differences in setup (physically separated slabs vs. blend) and electromagnetic modes (SP vs. microcavity). We argue that these differences do not preclude good agreement with respect to order of magnitude:

- The validity of comparing physically separated slabs and a blend of donors and acceptors has been explained in Section S3.3, as well as Section 3 of the main text.

- Energy-transfer rates (Eq. (11)) are dictated by energy gaps between polariton and dark states, exciton fractions of polariton states, and the spectral densities, regardless of the nature of the electromagnetic modes.

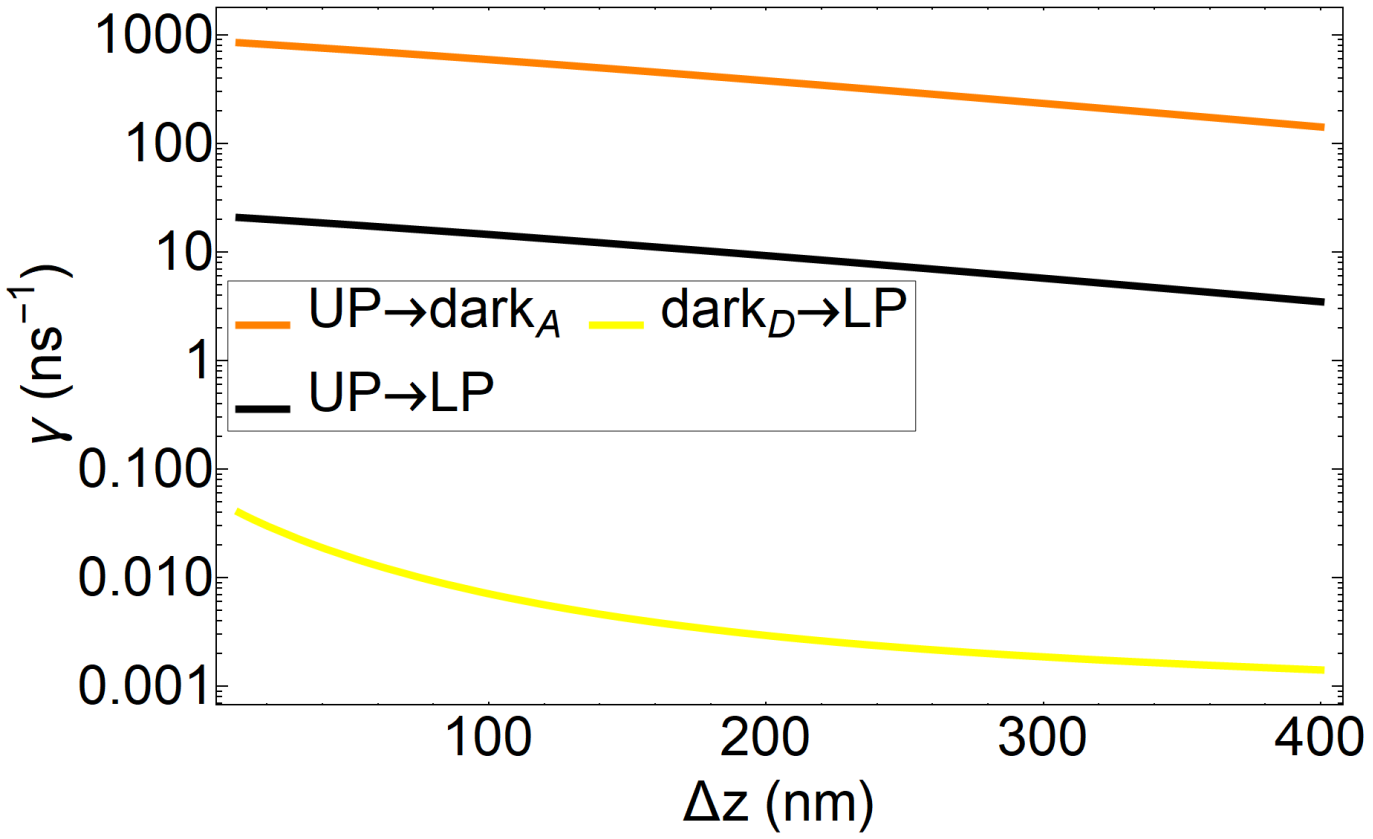

Fig. S5 SC of SPs to both donors and acceptors. EET rates (that are not shown in Fig. 4 of the main text) as a function of donor-acceptor separation Δz for downhill transtions among polariton and dark states. The SP mode is resonant with the donor transition, and the donor slab lies 1 nm from the metal and has fixed position while the acceptor slab is moved in the $+z$-direction to vary Δz.

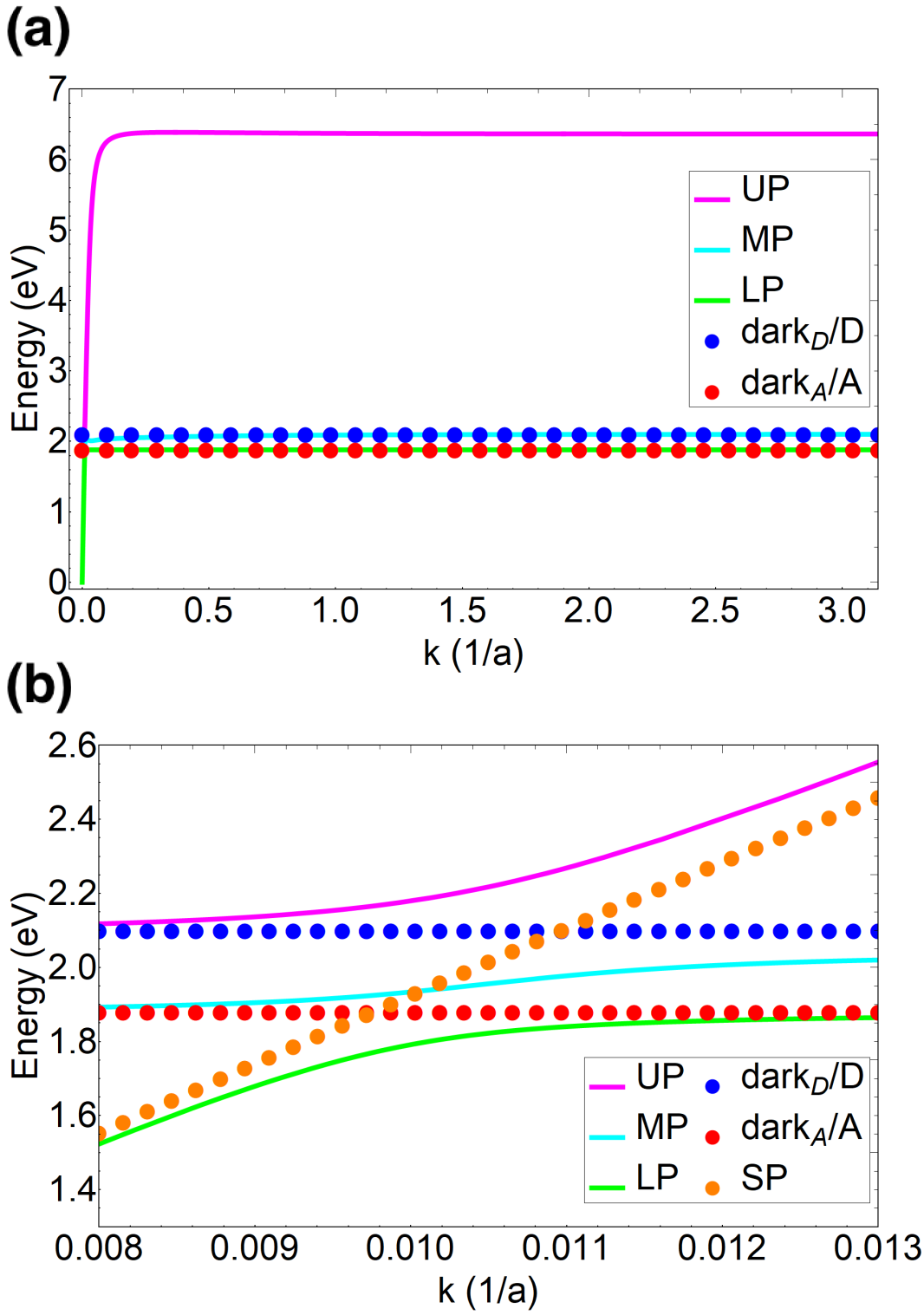

Fig. S6 SC of SPs to both donors and acceptors. (a) Dispersion curve in the FBZ. Donor-acceptor separation is 205 nm. The dispersion curves at all other donor-acceptor separations (10-400 nm) have the same qualitative form. The value $a = 1 \times 10^{-9}$ m is the inter-chromophoric lattice spacing for both donor and acceptor slabs. (b) Expanded view of dispersion curve at region of anticrossings characteristic of SC; the SP dispersion has been added to help visualize the anticrossings.

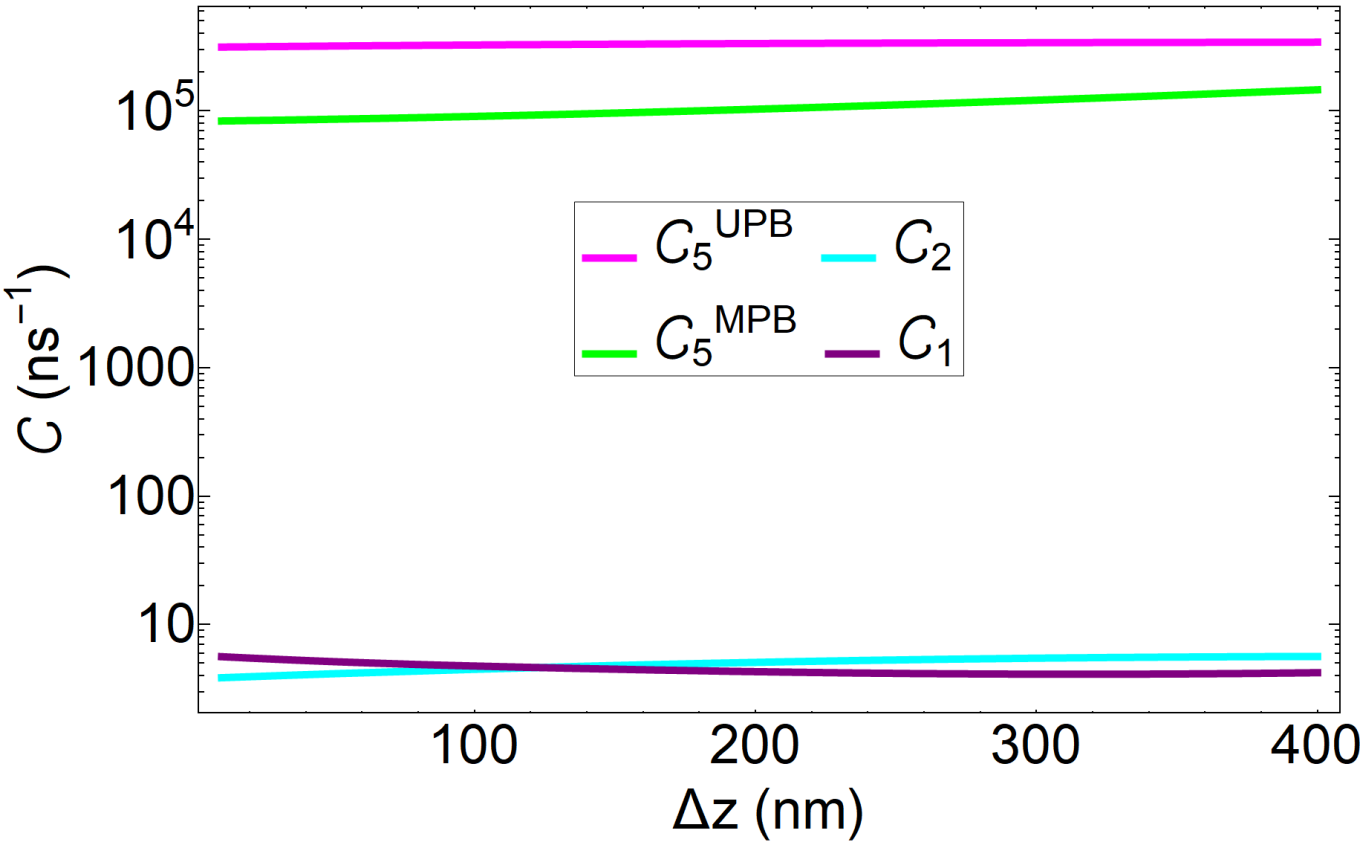

Fig. S7 SC of SPs to both donors and acceptors. Rate parameters $\mathscr{C}$ as a function of donor-acceptor separation Δz for downhill transitions. The donor slab lies 1 nm from the metal and has fixed position while the acceptor slab is moved in the $+z$-direction to vary Δz.

References

S1. L. Novotny and B. Hecht, *Principles of Nano-Optics*, Cambridge University Press, 2nd edn., 2012.

S2. A. Archambault, F. Marquier, J.-J. Greffet and C. Arnold, *Phys. Rev. B*, 2010, **82**, 035411.

S3. J. Yuen-Zhou, S. K. Saikin, T. Zhu, M. C. Onbasli, C. A. Ross, V. Bulovic and M. A. Baldo, *Nat. Commun.*, 2016, **7**, 11783.

S4. A. González-Tudela, P. A. Huidobro, L. Martín-Moreno, C. Tejedor and F. J. García-Vidal, *Phys. Rev. Lett.*, 2013, **110**, 126801.

S5. L. A. Martínez-Martínez, R. F. Ribeiro, J. A. Campos Gonzalez Angulo and J. Yuen-Zhou, *ACS Photonics*, 2017, **5**, 167–176.

S6. J. Yuen-Zhou, S. K. Saikin and V. Menon, *ArXiv e-prints*, arXiv:1711.11213.

S7. H. Sumi, *J. Phys. Chem. B*, 1999, **103**, 252–260.

S8. J. Ma and J. Cao, *J. Chem. Phys.*, 2015, **142**, 094106.

S9. H. Feshbach, *Ann. Phys.*, 1958, **5**, 357–390.

S10. H. Feshbach, *Ann. Phys.*, 1962, **19**, 287–313.

S11. S. Mukamel, *Principles of nonlinear optical spectroscopy*, Oxford University Press, 1995.

S12. M. Shapiro and P. Brumer, *Quantum Control of Molecular Processes*, Wiley, 2012.

S13. A. E. Cohen and S. Mukamel, *J. Phys. Chem. A*, 2003, **107**, 3633–3638.

S14. S. Lloyd and M. Mohseni, *New J. Phys.*, 2010, **12**, 075020.

S15. I. Kassal, J. Yuen-Zhou and S. Rahimi-Keshari, *J. Phys. Chem. Lett.*, 2013, **4**, 362–367.

S16. I. Medintz and N. Hildebrandt, *FRET - Förster Resonance Energy Transfer: From Theory to Applications*, Wiley, 2013.

S17. A. Govorov, P. L. H. Martínez and H. V. Demir, *Understanding and Modeling Förster-type Resonance Energy Transfer (FRET): Introduction to FRET*, Springer Singapore, 2016.

S18. D. M. Coles, P. Michetti, C. Clark, W. C. Tsoi, A. M. Adawi, J.-S. Kim and D. G. Lidzey, *Adv. Funct. Mater.*, 2011, **21**, 3691–3696.

S19. D. M. Coles, N. Somaschi, P. Michetti, C. Clark, P. G. Lagoudakis, P. G. Savvidis and D. G. Lidzey, *Nat. Mater.*, 2014, **13**, 712–719.

S20. P. Michetti and G. C. La Rocca, *Phys. Rev. B*, 2008, **77**, 195301.

S21. We associate the nomenclature of Coles et al. to ours to minimize the introduction of new names and variables: upper polariton band (UPB) $\rightarrow$ UP, middle polariton band (MPB) $\rightarrow$ MP, and lower polariton band (LPB) $\rightarrow$ LP, ex2 $\rightarrow$ donors (D), exciton reservoir ex2 $\rightarrow$ dark donors ($dark_D$), ex1 $\rightarrow$ acceptors (A), exciton reservoir ex1 $\rightarrow$ dark acceptors ($dark_A$).

S22. T. K. Hakala, J. J. Toppari, A. Kuzyk, M. Pettersson, H. Tikkanen, H. Kunttu and P. Törmä, *Phys. Rev. Lett.*, 2009, **103**, 053602.